ABSTRACT

Title of Thesis: ANALYZING TRENDS IN BENTHIC MACROFAUNAL BIODIVERSITY IN THE PACIFIC ARCTIC THROUGH TAXONOMINC AND GENOMIC METHODS

Nicholas John Silverson, Master of Science, 2025

Dissertation directed by: Professor, Dr. Jacqueline M. Grebmeier, Marine-Estuarine and Environmental Science

Trends and environmental parameters that can influence benthic macrofaunal biodiversity were examined at sites in the Distributed Biological Observatory, a group of time-series stations located in the biologically productive shallow Pacific Arctic shelf region. This goal of this study was to better understand the underlying drivers of biodiversity and connectivity, which are important for predicting regional ecosystem resiliency to future warming, especially as sea ice loss and seawater warming have impacted seasonal water column production, carbon export to the benthos, and benthic faunal community structure and composition. A mixed-effects regression analysis was undertaken on taxonomically-based Shannon Index macrofaunal data from 1998-2019 to identify the region-wide environmental parameters influencing benthic macrofaunal biodiversity and any temporal and spatial patterns of variability.

An index of the heterogeneity of sediment grain size classes, representing niche space, was found to positively influence biodiversity at both regional and sub-regional scales. There were few temporal trends in sediment heterogeneity, yet both positive and negative biodiversity trends

persisted at specific locations, related to other environmental parameters. Specifically, the length of seasonal sea ice persistence influenced biodiversity, but with some regional complexities. A phylogeographic analysis of three benthic macrofaunal species from the northern Bering and Chukchi Seas was conducted using cytochrome c oxidase (CO1) barcode data. The study examined two clam species, Ennucula tenuis (Montagu, 1908) and Macoma calcarea (Gmelin, 1791), along with the polychaete Cistenides hyperborea (Malmgren, 1866), to investigate population-level genetic connectivity in these seasonally productive, shallow-shelf ecosystems. Genetic barcode data were compared with sequences in National Center for Biotechnology (NCBI) from other studies across the Arctic to assess broader population dynamics. E. tenuis specimens belonged to a single population with distinct geographic variation. Analysis of M. calcarea was inconclusive due to technical problems during sample processing that prevented developing a population structure assessment prior to completing this thesis. C. hyperborea specimens from the northern Bering and Chukchi Seas formed a single population with two closely related haplotypes and minimal geographic genetic differentiation. However, sequences from this study differed significantly from Cistenides hyperborea records in the NCBI, suggesting there may be have taxonomic uncertainties associated with available data in the NCBI.

ANALYZING TRENDS IN BENTHIC MACROFAUNAL BIODIVERSITY IN THE PACIFIC ARCTIC THROUGH TAXONOMINC AND GENOMIC METHODS

by

Nicholas John Silverson

Thesis submitted to the Faculty of the Graduate School of the
University of Maryland, College Park, in partial fulfillment
of the requirements for the degree of
Master of Science
2025

Advisory Committee:

Professor Jacqueline M. Grebmeier, Chair
Professor Lee W. Cooper
Dr. Matthew Galaska

© Copyright by
Nicholas John Silverson
2025

Acknowledgments

First, I want to thank primary advisor, Dr. Jacqueline Grebmeier for her knowledge and support during my graduate studies. I would also like to thank my committee member, Dr. Lee Cooper, for his guidance and wisdom, especially as an editor. They both were approachable and insightful as they took the time to help me navigate the process of applying for a fellowship, an internship, and writing a research thesis, despite their many other obligations. They both encouraged me to follow my research interests and kept me on track. I learned much from them about all stages on the scientific process and I am grateful for the opportunity they gave me to travel to Alaska to participate in two research cruises. These experiences will stay with me throughout my life.

I also want to thank Dr. Matthew Galaska for mentoring me as an intern at the Pacific Marine Environmental Laboratory and serving on my advisory committee. He took time to personally teach me all stages of conducting a genetic study, which will serve me through my career, as well as advise me on various scientific career paths. These skills and his mentorship have been invaluable.

I want to thank Stephanie Soques and Alicia Clarke for teaching me taxonomic identifications and introducing me to the biodiversity of the Pacific Arctic benthos. They were patient with me and continued to support me with my taxonomic identifications and friendship throughout my time at CBL. I also want to thank Dr. Vyacheslav Lyubchich for statistical analysis conception and support. Additionally, thanks to Shannon Browne (NOAA PMEL) for genetic laboratory support. Thank you to Dr. Laura Rupprecht (University of North Carolina) for her invaluable support and advice throughout my graduate studies. Thanks to Erica Doo (DooStuff.com) for graphical support, especially with Adobe applications.

Lastly, I want to thank my partner, Jonathan, for all his support. I also would like to thank my friends and family, especially my mother, Kate Holz, my father, Don Silverson, my brother, Nat Silverson, and my sister-in-law, Eloise Meltzer. I couldn't have done it without all of their support.

Financial support was provided by NOAA CINAR (grant # 25984.02) and NSF (OPP-1917469) to JM Grebmeier and LW Cooper for recent field and synthesis activities. I was also supported by the National Science Foundation Graduate Research Fellowship Program under Grant No. 1840380 to N.J. Silverson, and an NSF INTERN Supplemental Grant for genomics work to NSF OPP-1917469.

Table of Contents

Acknowledgments ii
Table of Contents iv
List of Tables vi
List of Figures viii
List the Appendix tables and captions x
List the Supplementary files and captions xi
Chapter 1. Introduction—environmental conditions and associated drivers of benthic macrofaunal biodiversity in the Pacific Arctic 1
1.1 Overview 1
1.2 Macrofaunal Biodiversity in the Pacific Arctic 2
1.3 Key Environmental drivers of macrofaunal biodiversity 6
1.3.1 Water mass, sediment grain size and carbon content as key drivers of macrofaunal biodiversity 6
1.3.2 Seawater Temperature driven expansion 9
1.4 Water column and sea ice primary production 11
1.6 Contributions of genetic analyses to biodiversity studies 13
1.7 Thesis Goal, Objectives and Methods 14
Chapter 2. Environmental parameters influencing benthic biodiversity in the Pacific Arctic between 1998 and 2019 17
2.1 Introduction 18
2.1.1: Background and rationale 18
2.1.2 Study Objectives 20
2.2 Materials and Methods 21
2.2.1 Nomenclature 21
2.2.2 Data Collection 23
2.2.3 Regionwide Biodiversity Model Selection 24
2.2.4 Sub-regional benthic macrofaunal biodiversity 25
2.3 Results 26
2.3.1 Region-wide biodiversity 26
2.3.2 Dominance in each DBO sub-region 28
2.3.3 Biodiversity trends in each DBO sub-region 35
2.4 Discussion 42
Chapter 3. Pan-Arctic regional intraspecific genetic differences of three benthic macrofauna: *Ennucula tenuis*, *Macoma calcarea*, and *Cistenides hyperborea* 49

3.1 Introduction 50
3.1.1 Background and rationale 50
3.1.2 Study area 51
3.1.3 Study Objectives 52
3.1.4 Hypothesis 52
3.2 Materials and Methods 52
3.2.1 Data Collection 52
3.2.2 DNA Extraction and Qubit Analysis 55
3.2.3 PCR Preparation 55
3.2.4 DNA Purification, QC, and Sequencing 56
3.2.5 Bioinformatic Analysis 56
3.3 Results 57
3.3.1 *Ennucula tenuis* 57
3.3.2 *Macoma calcarea* 64
3.3.3 *Cistenides hyperborea* 65
3.4 Discussion 67
Chapter 4. Conclusions: approaching biodiversity in the Pacific Arctic through taxonomic and genetic lenses 73
4.1 Overview of thesis goals and key findings 73
4.1.1 Conclusions on Chapter 2: Environmental parameters influencing benthic biodiversity in the Pacific Arctic between 1998 and 2019 73
4.1.2 Conclusions on Chapter 3. Pan-Arctic regional genetic differences of three benthic macrofauna: *Ennucula tenuis*, *Macoma calcarea*, and *Cistenides hyperborea.* 74
4.2 Future Work 75
Appendices and supplementary section 78

List of Tables

Table 2.1. Historic station and current DBO stations names, latitude, longitude and length of occupation. Key: SLIP =St. Lawrence Island Polynya, UTBS=University of Tennessee Bering Strait, UTN=University of Tennessee Historical Stations, SEC=SE Chukchi Sea. 22

Table 2.2. Spearman's rho rank correlation analysis of Shannon index (SI) diversity for all DBO stations combined, as well as DBO sub-regions (DBOs 1-4) and UTN stations in the DBO3 region. Nearshore DBO3 (SEC) refers to SEC4-8. Columns 2-3 are water parameters, 4-7 are sediment parameters, and 8-10 are ice parameters. Bolded rho values indicate statistical significance ($p < 0.05$). 27

Table 2.3. Total organic carbon and total organic nitrogen were auto-correlated at the regional and sub-regional scale. In each case, the environmental parameter with the lower variance inflation factor (VIF) was used in further model building. 28

Table 2.4. The top 3 most abundant macrofaunal families at each site collected in July 2019. Each family is reported as a percent abundance in relation to the total organism abundance collected at each particular site. Faunal type listed in parentheses after family names, with key: A=Amphipods, B=Bivalves, C=Cumaceans, P=Polychaetes, E=Echinoderm. 29

Table 2.5. Summary of time series length, Student's T-tests, Mann Kendall tests, sieve bootstrapped T-tests, and sieve-bootstrapped Mann Kendall tests for SI at SLIP, UTBS, and UTN stations. Bold type and an asterisk indicate statistical significance ($p < 0.05$). 36

Table 2.6. Regional and sub-regional mixed effects models summarized. The regression coefficient (listed in parenthesis) is a measure of the strength of associated between the environmental influence and biodiversity. Sediment heterogeneity (the proportion of fine sediments to coarse sediments) corresponds to diversity of sediments and niches for benthic infauna. 44

Table 3.1. Standard nucleotide indices from Ennucula tenuis CO1 barcode data.....58

Table 3.2. Analysis of molecular variance statistics for Ennucula tenuis based on CO1 data.....58

Table 3. 3. Pairwise distance (Fst) Ennucula tenuis CO1 data between sub-regions.....58
Table 3.4. Standard nucleotide indices from CO1 barcode data for Ennucula tenuis from this study and across the Arctic. 60

Table 3.5. Analysis of molecular variance statistics for Ennucula tenuis based on CO1 data from this study and other data available from across the Arctic. 61

Table 3.6. Pairwise distance (Fst) between sub-regions based on Ennucula tenuis CO1 data from this study and studies across the north Pacific, Arctic, and North Sea. 62

Table 3.7. Standard nucleotide indices from Cistenides hyperborea CO1 barcode data.....65

Table 3.8. Analysis of molecular variance statistics for Cistenides hyperborea based on CO1 data. 66

Table 3.9. Pairwise distance (Fst) Cistenides hyperborea CO1 data between sub-regions. Bolded values indicate statistical significance ($p < 0.05$). 66

List of Figures

Figure 1.1. A map of five sampling regions of the Distributed Biological Observatory (DBO), which extends from the northern Bering into the Chukchi and Beaufort Seas and consists of decades-long occupied time series sites at hotspots of macrofaunal biological productivity. 4

Figure 2.1. Conceptual diagram illustrating that sediment heterogeneity can be expected to positively influences biodiversity as it corresponds to increased niche space. Sediment heterogeneity is the diversity of sediment grain sizes in an area. Gravel and coarse sand are larger sediments, while mud and silt are smaller sediment grain sizes. Macrofaunal biodiversity will be highest at sites with high bottom sediment heterogeneity, represented by a larger range of sediment grain sizes. Because different animals are associated with different sediment types, higher sediment heterogeneity corresponds to increased niche space.....21

Figure 2.2. Abundance trend of dominant faunal groups at SLIP1 stations (DBO1) from 2000-2019. 29

Figure 2.3. Abundance trend of dominant faunal groups at UTBS stations (DBO2) from 1999-2019. 32

Figure 2.4. Abundance trend of dominant faunal groups at UTN stations (DBO3 region) from 1998-2019.....33

Figure 2.5. Abundance trend of dominant faunal groups at SEC stations (DBO3) from 1993-2019. 34

Figure 2.6. Abundance trend of dominant faunal groups at DBO4 stations from 2013-2019. Note from 2013-2017 the original DBO4 stations were located south of the new DBO4n sites that were relocated further north in 2018-2019 and likely impact the evaluation of the trend. 35

Figure 2.7. Increasing Shannon index trends in DBO1 at SLIP1(A) (Mann-Kendall tau = 0.46, $p < 0.001$) and SLIP 5 (B) (Mann-Kendall tau = 0.4, $p < 0.001$). Gray line shows data and blue line shows a moving average of 3 years to provide for trend visualization. 37

Figure 2.8. Surface sediment heterogeneity (A-B) and sea ice breakup date (C-D) trends at SLIP 1 and SLIP 5. Sea ice breakup date is defined as the day of the year (DOY) that ice fell below a 15% sea ice concentration threshold. SLIP1 had no trend in sediment heterogeneity, but a significant trend (Student's t value = -2.0097, $p < 0.05$) for an earlier ice breakup date. SLIP5 also had no trend in sediment heterogeneity, but a trend existed (Student's t value = -2.2249, $p < 0.05$) for an earlier ice breakup date. Gray line shows data with the blue line shows a moving average of 3 years to facilitate trend visualization. 37

Figure 2.9. Increasing Shannon index trends at UTBS2 (A) (Mann-Kendall tau = 0.61, $p < 0.001$) and UTBS4 (B) (Mann-Kendall tau = 0.62, $p < 0.001$). 38
Figure 2.10. Declining trends in sea ice persistence at UTBS2 (Mann-Kendall tau = -0.446, $p < 0.001$) and UTBS4 (Mann-Kendall tau = -0.438, $p < 0.001$). Gray line show data with the blue line shows a moving average of 3 years to provide for trend visualization. 39

Figure 2.11. Increasing Shannon index trends at UTN3 1(A) (Mann-Kendall tau = 0.38, $p < 0.001$) and UTN5 (B) (Mann-Kendall tau = 0.43, $p < 0.001$). Sea ice breakup date is defined as the day of the year that ice falls below a 15% sea ice concentration threshold, based upon satellite observations. The gray line indicates individual station data. The thicker blue line shows a moving average of 3 years of values at stations. 40

Figure 2.12. Shannon index had a decreasing trend at SEC2 (A) (Student's T-value = -0.06, $p < 0.05$) and there was no significant trend in sediment heterogeneity at the same site (B). The gray line shows data values with the blue overlaying line shows a moving average of 3 years. 41

Figure 3.1. A. A map of collection locations of Ennucula tenuis, Macoma calcarea, and Cistenides hyperborea specimens analyzed for population genetics, including sources of CO1 data obtained from the National Center for Biotechnology Institute (NCBI). Major sub-regions include the north Pacific, the northern Bering and Chukchi Sea combined, the Beaufort Sea, and the Hudson Bay, the North Sea, and the White Sea. B. Green circles indicate collection locations for specimens in this study. Station IDs: DBO=Distributed Biological Observatory, SLIP=St. Lawrence Island Polynya, UTBS=University of TN Bering Sea, and LB=Ledyard Bay.....54

Figure 3. 2. Median-joining haplotype network based upon CO1 sequences for Ennucula tenuis. The size of circle represents how many specimens fit into each particular haplotype. Haplotypes are colored by location. Notches between haplotypes represent one single nucleotide polymorphism. 59

Figure 3.3. A scatterplot of genetic (pairwise F_{st}) and geographic distance (kilometers) of Ennucula tenuis specimens from the DBO region and across the Arctic. A red regression line to visualize trend is plotted. 64

Figure 3.4. Median-joining haplotype network based upon CO1 sequences for Cistenides hyperborea. The size of circle represents how many specimens fit into each particular haplotype. Haplotypes. Notches between haplotypes represent one single nucleotide polymorphism (SNP). 67

List the Appendix tables and captions

Table A1. Sample locations, abbreviations, samples sizes, and collectors of *Ennucula tenuis, Macoma calcarea,* and *Cistenides hyperborea* used in a CO1 DNA barcode analysis. For further information on specimen collections, including cruise and year of collection, refer to supplementary file: **S2. Silverson_popgen2023.csv**.

Table A2. Results of a Basic Local Alignment Search Tool (BLAST) algorithm search in the NCBI database for *Macoma calcarea* specimens. Results indicated contamination of DNA sequences of *M. calcarea*.

List the Supplementary files and captions

S1_Silverson_DBO_diversity2000_2019.csv contains all data used for the statistical analysis of biodiversity in Chapter 2. This data includes Shannon Index, environmental parameters, including sediment variables, from SWL cruises to DBO sites from 2000-2019. Original data available at https://arcticdata.io/catalog/portals/DBO/Data

S2_Silverson_popgen2023.csv lists all collection data for *E. tenuis*, *M. calcarea*, and *C. hyperborea* specimens used in population genetic analyses.

S3_Silverson_e_tenuis_DNA.fasta is a list of aligned and edited DNA for *Ennucula tenuis* specimens.

S4_Silverson_m_calcarea_DNA.fasta is a list of aligned and edited DNA for *Macoma calcarea* specimens. Results indicated contamination of DNA sequences of *M. calcarea* and were inconclusive.

S5_Silverson_c_hyperborea_DNA.fasta is a list of aligned and edited DNA for *Cistenides hyperborea* specimens.

S6_Silverson_NCBI_DNA.fasta is a list of aligned and edited DNA for specimens collected that were not present in the NCBI database, including *Liocyma fluctuosa* (Gould, 1841), *Ocnus glacialis* (Ljungman, 1879), and *Pelonaia corrugata* (Goodsir and Forbes, 1841). Results indicated contamination of DNA sequences of these specimens and were inconclusive.

S7_SWL19_dominance.csv. Summary data as example of dominant benthic macrofaunal for SWL19; original benthic macrofaunal data set available at https://doi.org/10.18739/A2PN8XG88.

S8_Silverson_SWL23_table2023.csv. A summary table of taxa samples for DNA analysis collected on the SWL23 cruise.

S9_Silverson_SKQ202312s_table2023.csv. A summary table of taxa samples for DNA analysis collected on the SKQ2023 cruise.

Chapter 1. Introduction—environmental conditions and associated drivers of benthic macrofaunal biodiversity in the Pacific Arctic

1.1 Overview

The rapid warming of the Arctic Ocean is causing a decline in sea ice (Osbourne et al., 2017; Frey et al. 2023). This decline is occurring both in terms of duration (earlier melt and later freeze- up) (Meier et al., 2014; Frey et al. 2023) and thickness; multiyear ice has declined and been replaced with thinner, first-year ice (Post et al., 2009; Maslanik et al., 2011). These changes, in tandem with warming seawater, have consequences for patterns of abundance, species richness, and biodiversity as subarctic species formerly limited by sea ice or cold waters expand their ranges northward. The northward expansion of subarctic species ranges has been termed borealization (Carmack and Wassmann, 2006). In marine systems, it is often driven by the advection of warmer, subarctic waters into the Arctic basin (Polyakov et al., 2020) and by regional warming seawater and reduced sea ice, which have historically been barriers to range expansions of subarctic species (Renaud et al., 2015). These range expansions have consequences for benthic and pelagic community composition, especially as novel species affect long-standing ecosystem patterns of abundance (Pecuchet et al., 2020). Reduced sea ice and associated changes in biological communities could also alter marine productivity (Arrigo and van Dijken, 2015) and biogeochemical cycling (Lannuzel et al. 2018), which can have further effects on community composition and biomass. Understanding how these range expansions, as well as changes in sea ice and ocean temperature, will affect Arctic Ocean ecosystem structure has major implications for gauging the resiliency of benthic species to current and future warming.

While predicted changes in environmental drivers are clear, how the biodiversity of benthic macrofauna will respond is more complex and likely will be taxon and habitat-dependent

(Renaud et al., 2015; Renaud et al. 2019), with potentially few certain Arctic-wide trends. For example, Mueter et al. (2021) associated a decrease in benthic species diversity and an increase in zooplankton and demersal fish diversity with warmer waters. But these shifts of biodiversity may have been temporary and spatially variable, as interactions between resident and invading species have unclear consequences, both through biological competition and habitat variability. Consequences of the range expansions of subarctic fauna include the potential for the northward retreat or even extirpation of Arctic endemics. Specific life history traits of benthic taxonomic groups (e.g. benthic or pelagic dispersal stages) will influence expansion and retraction in the altered physical oceanography of an ice-free Arctic (Renaud et al., 2015). Biological species changes are likely to be seen among all habitat types, but for sessile, benthic macrofauna, range expansions might be primarily limited to a larval dispersal stage, which are dependent on physical drivers like currents (Ershova et al., 2019). Furthermore, sessile, long-lived benthic macrofauna respond to overall water column processes influencing productivity (Grebmeier et al., 2018) and so understanding changes in benthic community composition can provide insights into the overall ecosystem response.

1.2 Macrofaunal Biodiversity in the Pacific Arctic

The Distributed Biological Observatory (DBO) consists of some time series benthic stations that have been repeatedly sampled for decades in the Pacific Arctic (Grebmeier et al. 2006a, 2018; Fig. 1.1). Based upon this sampling, the region south of St. Lawrence Island, where an area of open water in ice covered seas, or a polynya, forms each winter (hereafter referred to as the SLIP region) has historically had stations dominated by nuculanid and nuculid bivalves. However, recently the southernmost sampling area of the SLIP (SLIP 1-3 stations) has shifted to maldanid polychaetes, with an accompanying decline in overall biomass (Grebmeier et al., 2018). The northernmost portion of this region has remained dominated by nuculanid and

nuculid bivalves (occasionally tellinid bivalves), with persistent high biomass (Grebmeier et al., 2018). This northern region of the Bering Sea has some of the longest periods of open water in the region, but associated annual primary production rates are mid-range due to a decline in nutrient availability in summer months after the spring phytoplankton bloom (Springer et al. 1996). However, overall annual rates of primary productivity have increased in the SLIP region from 2003-2020 (37.7 g C/m^2/year/decade), based upon satellite observations (Frey et al., 2023).

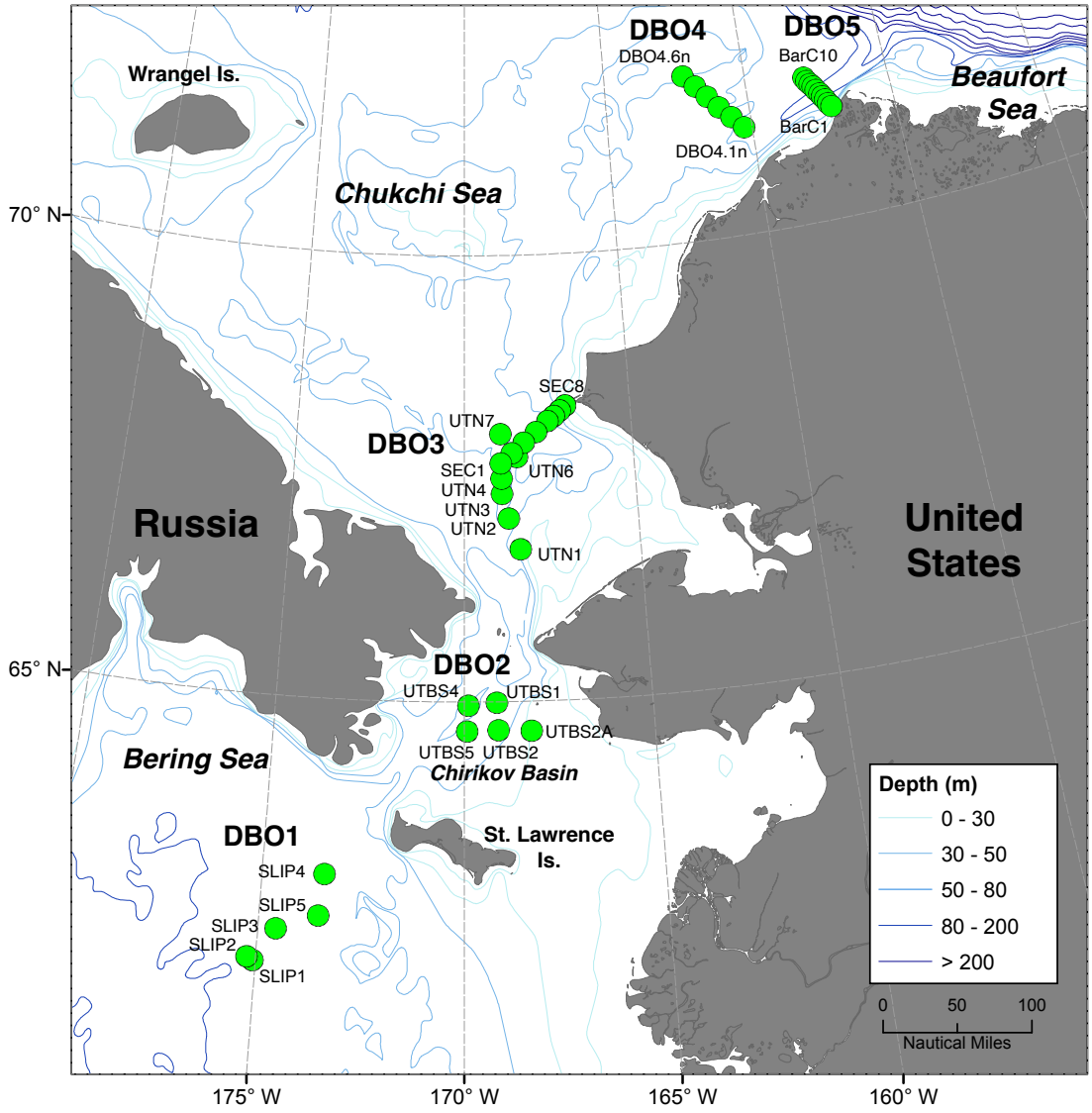


Figure 1.1. A map of five sampling regions of the Distributed Biological Observatory (DBO), which extends from the northern Bering into the Chukchi and Beaufort Seas and consists of decades-long occupied time series sites at hotspots of macrofaunal biological productivity.

The Chirikov Basin, north of St. Lawrence Island and south of the Bering Strait (sampling region hereafter referred to at UTBS) was historically dominated by ampeliscid amphipods, with varying biomass driven by the different water masses associated with the nutrient-rich Anadyr Current in the west and the nutrient-poor Alaska Coastal current in the east. Biodiversity is low due to homogenous sandy sediments composed of fine and very fine sand

(Grebmeier et al., 1989). The western nutrient-rich waters, with nutrients available through much of the open water period, have supported some of the highest levels of primary productivity in the region. However, from 2003-2020, annual primary productivity as observed from satellite platforms did not significantly increase, and there were observed negative trends in June primary productivity (-354 mg/m^2/day/decade) and positive trends in September (338 mg/m^2/day/decade), suggesting changes in the timing of phytoplankton blooms (Frey et al., 2023). By 1999, the east (UTBS 1-2 stations) continued to be dominated by ampeliscid amphipods, but the southwest (UTBS5 station) was dominated by ampharetid polychaetes and the northwest (UTBS4 station) was dominated by nuculid bivalves. Biomass in the eastern region at UTBS 1-2 stations declined from 2002-2010 and then increased to 2015. Biomass in the northwest at the UTBS4 station declined from 2002-2015 and biomass at UTBS5 station in the southwest increased from 1996-2006, subsequently declining until 2015 (Grebmeier et al., 2018).

The southeast Chukchi Sea (sampling sites here are referred to as the UTN stations) was historically dominated by tellinid bivalves, namely *Macoma calcarea*, Gmelin, 1791, and to a lesser extent by amphipods (Grebmeier et al., 2006a, 2018; Sirenko and Gagaev, 2007). This area has historically had higher diversity than the Chirikov Basin, associated with heterogeneous sediments (Grebmeier et al., 1989). By 1999, station UTN1 in the southernmost part of the region transitioned to dominance by sand dollars *Echinarachinius parma*, Lamarck, 1816 in sandy sediments, which continues through the present day. The remaining part of the region (UTN2-7 stations) from 1999 to present continued to be dominated by tellinid bivalves, but the northernmost portion (UTN6-7) had an increase in amphipods starting in 2012. The entirety of the region saw an increase in benthic biomass from 2010-2015 (Grebmeier et al., 2018). Annual primary productivity rates here are the highest in the Pacific Arctic region, with especially high rates in the spring caused by nutrient-rich, stratified water, which allows phytoplankton to use

nutrients and sunlight to build biomass. Annual primary production values observed from satellite platforms increased from 2003-2023 in the DBO3 region (48.0 g C/m^2/year/decade) (Frey et al., 2023).

The central and western Chukchi Sea regions are dominated by maldanid, lumbrinerid, and nephtyid polychaetes, as well as brittle stars and sipunculids (Grebmeier et al. 2006a). Community composition of the northern Chukchi Sea is influenced by varying nutrient concentrations in each water mass, as well as the degree of stratification, leading to variable patterns of biodiversity (Feder et al., 1994; Grebmeier et al., 2006a). The northeastern Chukchi Sea has parts dominated in biomass by bivalves and other parts dominated by amphipods (Blanchard et al., 2013; Grebmeier et al., 2006a).

1.3 Key Environmental drivers of macrofaunal biodiversity

1.3.1 Water mass, sediment grain size and carbon content as key drivers of macrofaunal biodiversity

Renaud et al. (2019) noted that there was limited evidence that the Arctic benthos is more sensitive to climate warming than the benthos in other regions. Specifically, they explored the intuitive expectation that as the Arctic warms, benthic boreal taxa will expand their ranges north. This study proposed that basic life history and physiological information on Arctic benthic taxa could assist management strategies, by predicting potential sites and habitats susceptible to invasive species. Their modeling output raises the point that shifting patterns of biodiversity and community composition are not homogenous across taxonomic groups and might be a result of many interacting drivers influencing community structure.

Many studies have attributed community structure in this region to water mass, which is influenced by multiple, interacting environmental drivers (Feder et al., 1994; Feder et al., 2006; Grebmeier et al., 1989, 2006a; Sirenko and Gagaev, 2007; Waga et al., 2020). The Pacific Arctic

is influenced by currents flowing northward through the Bering Strait, differentiated by two distinct water masses. The Anadyr Current flows north on the western side of the northern Bering and Chukchi Seas and is nutrient rich with a generally higher salinity (≥32.5 psu) and lower summer temperature (-1.0 to 1.5°C). In the eastern part of the northern Bering and Chukchi Seas, Alaskan coastal waters flow northward and in the summer are generally less saline (≤31.8 psu) and warmer (≥4°C). In the central northern Bering and Chukchi Seas, the two water masses mix, with summer salinity (31.8-32.5 psu) and temperature (0-1.5°C) in between those of the two distinct masses (Coachman, 1968; Grebmeier et al., 2006a). Grebmeier et al. (1989) found higher macrofaunal benthic diversity in the Pacific Arctic in the Alaska Coastal Water, which was less productive, warmer (in summer) and generally had a greater variety of sediment size classes. Lower macrofaunal diversity was found in the colder, highly productive water column regions influenced by Anadyr water that had more homogenous sediments and characterized by few, more dominant species.

Waga et al. (2020) associated benthic community change in the Bering and Chukchi Seas with altered current patterns. They found evidence for a potential regime shift in soft bottom biological communities, namely an increase in the number of macrofaunal families in the area south of the St. Lawrence Island polynya from 2000-2013 with increased northward water volume transport. This increase in family richness was not associated with an increase in Shannon diversity, based on abundance, implying that the increase in family-level richness did not affect overall biodiversity. Waga et al. (2020) concluded that invading species potentially have not yet been established in these communities. By contrast, macrofaunal family richness in the Southeast Chukchi Sea did not increase over this time period and the Shannon Index decreased.

Sediment type is another important driver of macrofaunal biodiversity in the Arctic, with higher biodiversity occurring generally in areas with heterogeneous bottom sediments (Grebmeier et al., 1989; Feder et al., 1994). Prior research found sediment heterogeneity, in addition to temperature and food supply, drove the community composition of Arctic benthic macrofaunal communities in the Pacific Arctic. Specifically, these prior studies found that high diversity in the Chukchi Sea was associated with a more heterogeneous mixture of silt, clay, sand, and gravel sediments (Mueter et al., 2021). Diversity was lower in the northern Bering Sea north of St. Lawrence Island (Fig. 1.1), which had more uniformly sandy, homogenous sediments. Additionally, these two prior studies associated substrate type to current speed; locations with higher current speeds are associated with coarser sediments as finer sediments remain suspended at higher speeds. These patterns of substrate type and current speed associated with community composition are found among other benthic shelf organisms at other Arctic locations (Roy et al., 2014; Iken et al., 2020).

Different sediment types are associated with different functional groups, for example coarse sediments are typically associated with higher current rates and suspension feeding animals, while finer sediments are associated with deposit feeders (Pisareva et al., 2015). It stands to reason that areas with multiple sediment types will support a greater variety of niches and benthic biodiversity will be amplified. Lin et al. (2019) found sediment grain size to be one of the most important drivers of benthic functional diversity. For example, that study found that both macrobenthic epifauna and infauna living in association with predominantly sandy sediments in the northeastern Bering Sea shelf were primarily surface dwelling mobile carnivores and scavengers. The siltier sediments of the southwestern Bering Sea contained semi-mobile deposit feeders and tube dwellers. Furthermore, Lin et al. (2019) found a linear relationship between functional diversity and the Shannon diversity of benthic organisms, which

they interpreted to indicate that there was little functional redundancy in shallow shelf benthic populations. They posited that these communities were at risk to regime shifts as the loss of a species could mean the loss of a functional group.

1.3.2 Seawater Temperature driven expansion

Many studies have hypothesized and found evidence that warming seawater has influenced dramatic shifts in Arctic benthic community composition. Over geological time-frames, species invasions in the Arctic have been associated with warmer temperatures (Vermeij and Roopnarine, 2008). Renaud et al. (2015) explored the idea that the warming Arctic would be more susceptible to invasion and they highlighted mechanisms of potential invasion in the Arctic benthos in the Atlantic Arctic and subarctic regions. They found widespread evidence that temperature thresholds of benthic fauna imply northward range constrictions for Arctic benthic fauna and expansions for boreal benthic fauna.

Patterns highlighted in Renaud et al. (2015) have been found elsewhere in the Pacific Arctic, where shifts in community composition coincided with warming waters (Blanchard et al., 2013; Grebmeier et al, 2018; Mueter et al., 2021). Arctic benthic macrofauna have exhibited northward shifts and reductions in abundance and biomass because subarctic species are no longer encountering temperature barriers. Mueter et al. (2021) compared changes in the diversity of different taxonomic groups, including macroinfauna, between two cruises in 2015 and 2017, respectively, in the Chukchi Sea; these two years had marked differences in water temperature and salinity. They found that warmer, more saline waters were associated with lower abundance and species richness in the benthos and higher abundance of demersal fish and zooplankton. They concluded that these conditions were consistent with borealization, namely a northward shift in subarctic species.

Blanchard et al. (2013) found that benthic density, biomass, and taxonomic diversity in the northeastern Chukchi Sea was negatively correlated with depth and bottom water temperature. Overall, they found benthic community structure to be driven by bathymetric control of water flow, which influences food supply and larval dispersal. This finding is corroborated by other Arctic studies, which attribute community composition to water mass characteristics and patterns (Feder et al., 1994; Feder et al., 2006; Grebmeier et al., 2006a; Sirenko and Gagaev, 2007). Water flow, influenced by seafloor topography and wind forcing, in turn affects organic matter availability to the benthos, resulting in high biomass communities in areas where organic matter readily exported to the benthos.

Grebmeier et al. (2018) noted northward shifts in total high macrofaunal biomass as well as changes in the dominant macrofaunal composition at offshore shelf sites in the Bering Strait region from 1998 to 2015. They attributed changing biomass patterns and community structure to marked declines in sea ice and warming waters over the period. Specifically, they found declines of previously dominant clam types in sites south of St. Lawrence Island coincided with an increase in polychaetes. In the Chirikov Basin, north of St. Lawrence Island in the Bering Sea, they found that a once high biomass of ampeliscid amphipods was no longer present, but populations had increased to the north and northeast. In the southeast Chukchi Sea, bivalve biomass increased from south to north at time series sites over the period from 2000-2018. These changes in biomass patterns have implications for higher trophic-level benthic feeding animals, such as spectacled eiders (listed as threatened under the US Endangered Species Act), gray whales, and Pacific walruses. Due to the ongoing environmental changes in the region, there is a suggestion that influence of the benthos might decline and be replaced with greater pelagic influence (Moore and Stabeno, 2015), constituting an ecosystem regime shift as projected in

Grebmeier et al. (2006b). How this shift in macrobenthic biomass relates to community composition and biodiversity patterns will be more formally explored in this thesis.

1.4 Water column and sea ice primary production

Benthic-pelagic coupling in the form of unconsumed pelagic organic matter exported to the benthos has defined the spatial variability of benthic communities in the Pacific Arctic continental shelf (Grebmeier et al., 2006a). Accordingly, understanding changes in the patterns of biodiversity in primary producers may drive the resulting changes in benthic community composition. However, the mechanisms and consequences in this shift at the base of the food web are unclear (Lannuzel et al. 2020).

Perhaps most importantly, warming waters and reduced sea ice extent eventually will lead to a decline in habitat for sea ice algae, an important primary producer in the Arctic (Koch et al., 2020). Ice algae occupy an important niche, and their potential extirpation in an ice-free Arctic could have a profound impact on the functional diversity of this ecosystem (Post et al., 2009). Sea ice algae are found at highest concentrations on the undersides of sea ice when enough sunlight can penetrate. As sea ice melts earlier, freezes later, and multi-year ice declines, more sunlight will penetrate the upper ocean. Sympagic algae are additionally found in pools of meltwater and in brine channels within the ice. Sunlight is a primary driver of sea ice algal primary producer community composition (Polyakov et al., 2020; Lannuzel. et al., 2020). Increases in ocean temperature also have had effects on ecosystem structure, primarily affecting metabolism (Polyakov et al., 2020). Koch et al. (2020) found a decline in a sympagic ice algal biomarker (highly branched isoprenoids) in the surface sediments in the northeast Chukchi Sea in the Pacific Arctic from 2012-2017, which coincided with declining ice on a spatial basis. These authors also found an increasing gradient of sympagic ice algal biomarkers northward, consistent with higher ice extent and duration.

As ice thins, increases in sympagic production associated with increased sunlight penetration might reasonably be expected. As ice continues to decline, eventually there might not be enough ice to support sympagic algal populations. Lannuzel et al. (2020) highlighted an additional concern as populations of consumers and ice algal producers could grow asynchronously. Changes in the structure, timing, and distribution of key primary producers would drive further community composition change with impacts further up the food chain.

While declines in ice thickness could support higher populations of sea ice algae, it could also support higher biomass of phytoplankton. For example, Arrigo et al. (2012) documented an under-ice bloom on the Chukchi Sea continental shelf dominated by widespread pelagic planktonic diatoms able to photosynthesize due to reductions in ice thickness. Similarly, Assmy et al. (2017) documented a time series sequence following the growth of an under-ice phytoplankton bloom of *Phaeocystis pouchetti* north of the Fram Strait in the Atlantic Arctic from winter to spring in 2015. The bloom was driven by leads within the ice cover and additionally occurred in the presence of snow cover on the sea ice surface, meaning that production could not be accurately estimated from satellite imagery.

Primary production in the Pacific Arctic during the open water period dominates annual production (Arrigo and van Dijken, 2015; Frey et al. 2023). Production varies on individual annual cycles and depending upon nutrient availability and light. In the Distributed Biological Observatory (DBO), the highest annual primary production value based upon satellite observations occur in DBO2 (238.7 g C/m^2/year) and DBO3 (214.5 g C/m^2/year), driven, in part, by nutrient rich waters in the western Bering Strait. The lowest values occur at DBO4 (88.3 gC/m^2/year) and middle-range values occur at DBO1 (144.5 g C/m^2/year) (Frey et al., 2023). While nutrient availability is an important factor for determining chlorophyll biomass, the number of open water days with enhanced light availability to surface waters, which is driven by

declining sea ice, was found to be the greatest factor contributing to increased regional primary production (Arrigo and van Dijken, 2015; Frey et al., 2023). Arrigo and van Dijken (2015) estimated an annual net phytoplankton primary production increase of 53% on the interior shelf of the Beaufort Sea and 28% on the inflow shelf of the Chukchi Sea from 1998-2012. As sea ice declines, more organic carbon will be fixed in the Pacific influenced Arctic Ocean, although water column stratification caused by surface warming could limit nutrient availability to support phytoplankton blooms.

1.6 Contributions of genetic analyses to biodiversity studies

The Arctic Ocean and adjacent seas have been conventionally thought of as species-poor, but recent studies have found intermediate levels of biodiversity compared with the global average (Hardy et al., 2010). This variable biodiversity is a result of complex and often species-specific evolutionary and life-histories (Renaud et al., 2015). The Bering Strait has influenced these evolutionary histories as it has been both a pathway and barrier to the dispersal of organisms from the North Pacific across the Arctic Ocean to the North Atlantic over glacial-interglacial time periods; the repeated openings and closings of the Bering Strait have influenced the complex history of Arctic marine biodiversity and the patterns of benthic biodiversity seen today (Vermeij and Roopnarine, 2008; Carr et al. 2011).

This revised thinking of the state of biodiversity in the Arctic has also been enabled by advances in molecular tools that have allowed for more efficient sequencing of DNA. Genetic data can inform morphologically based taxonomy. In particular, this approach can help resolve species complexes when there is a lack of morphological differences typically used to separate species. In the Arctic, DNA barcoding has revealed that some polychaetes and mollusks species that can be distinguished on morphological features were actually complexes of unrecognized species, indicating that biodiversity has been previously underestimated (Carr et al., 2011;

Layton et al. (2014). In cases where morphology is complex or taxonomic expertise is limited, genetic data, and particularly DNA barcoding, can be an effective solution (Hebert et al., 2003).

Unlike morphologically based taxonomy, genetics can also give insight into intraspecific diversity, i.e. population genetics, which can provide a different approach to biodiversity. Population genetics is a valuable tool for understanding the dynamics of organisms within an ecosystem. Specifically, it can reveal patterns of connectivity and isolation influenced by environmental factors, which can help identify geographic or oceanographic barriers to gene flow (Galaska et al., 2017). Population genetics can also describe the genetic diversity within or among populations, which can give insight into a population's ability to adapt to environmental change (Frankham, 2005). This insight can be important for designing conservation efforts in threatened areas. In the Pacific Arctic DBO region, due to benthic-pelagic coupling, benthic macrofaunal communities are important sentinels of the overall water column (Grebmeier et al., 2018; Moore and Stabeno, 2015). Examining population level genetics of dominant benthic macrofauna in the region could enhance knowledge of ecosystem dynamics.

1.7 Thesis Goal, Objectives and Methods

The overall goal of my thesis research was to investigate changes in Pacific Arctic macrofaunal biodiversity that have occurred over the last 20 years and to evaluate key environmental drivers of that change using time series data in the region. I chose to use the time-series statistical modeling approach facilitated by use of the Shannon Index (SI) (Shannon, 1948). Based on communication theory, SI is an index of biodiversity that has traditionally been used to summarize overall community diversity by taking into account each species' proportional composition to the overall ecosystem (Good, 1953; Margalef, 1967). It can be applied to both fine and large-scale taxonomic levels or genomic data (Konopiński, 2019).

I used both a statistical time series approach, which examined interspecific diversity, paired with a population genetic analyses of the bivalves *Ennucula tenuis* and *Macoma calcarea*, and a polychaete, *Cistenides hyperborea.* All three species are dominant constituents of benthic macrofauna that can provide insight into biodiversity change and related drivers over time. I chose to use the sampling infrastructure of an existing project, the DBO, which has had time series macrofaunal collections that provided an appropriate test bed for studying climate impacts on the biodiversity of benthic macrofaunal on the Pacific Arctic shelves. The DBO consists of marine time series sites from the northern Bering Sea to the Beaufort Sea designed to document and evaluate biological changes along a latitudinal gradient at productive regions (Moore and Grebmeier, 2018).

This thesis is an examination of the macrofaunal biodiversity in the DBO regions from the northern Bering Sea to the northern Chukchi Sea, using both taxonomic and genetic approaches. Chapter 2 is a statistical analysis of trends in macrofaunal biodiversity using time series analysis based on faunal taxonomy. I test two hypotheses using both macrofaunal population and environmental data collected over two decades in the Pacific Arctic:

H1: Higher bottom water temperatures lead to higher macrofaunal biodiversity in the continental shelves of the Pacific Arctic, specifically the northern Bering and Chukchi Seas.

H2. Macrofaunal biodiversity will be higher at sites with more heterogeneous bottom sediment types, meaning a range of sediment grain sizes. The increased niche space of multiple sediment habitats will support higher station diversity (Kędra and Grebmeier, 2020).

Chapter 3 provides a pilot-level analysis of finer-scale patterns of biodiversity, derived from benthic macrofaunal samples collected in 2023 and using genetic analysis to characterize population structure.

H3: DNA barcoding will detect different populations of select dominant benthic macrofauna.

Chapter 4 integrates and synthesizes potential outcomes for macrofaunal biodiversity change, both at the intra- and inter-specific level, as the Pacific Arctic warms and longstanding oceanographic drivers are potentially altered.

Chapter 2. Environmental parameters influencing benthic biodiversity in the Pacific Arctic between 1998 and 2019

Abstract

Trends and environmental parameters that can influence benthic biodiversity were examined at sites in the Distributed Biological Observatory, a group of time-series stations located in the biologically productive shallow Pacific Arctic shelf region. A mixed-effects regression analysis was undertaken on taxonomically-based Shannon Index macrofaunal data and parallel environmental data collected from 1998-2019 to identify region-wide environmental parameters influencing benthic macrofaunal biodiversity and any temporal and spatial patterns of variability. An index of the heterogeneity of sediment grain size classes, a functional measure of niche space, was found to positively influence biodiversity at both regional and sub-regional scales. There were no trends in sediment heterogeneity over time, but both positive and negative biodiversity trends persisted at specific sub-regional locations, and also related to other environmental parameters, particularly sea ice persistence. The length of seasonal sea ice persistence influenced biodiversity sub-regionally, with some variability. As sea ice loss and warming waters are predicted to continue to increase in coming years, the impact of these key environmental indicators may become more explicit. Additionally, if current patterns are modified as a result of warming or increased fresh water input into the Arctic from Pacific sources, the distribution of sediment size particle classes could change, altering patterns of biodiversity.

2.1 Introduction

2.1.1: Background and rationale

Biodiversity is complex, and influenced by environmental parameters that vary on spatial and temporal scales. In Pacific Arctic macroinfaunal benthic systems, sediment grain size plays an important role in determining community composition, with more heterogenous, poorly sorted sediments associated with higher diversity (Grebmeier et al., 1989; Feder et al. 2007). Areas of high biodiversity are often associated with nutrient poor, less productive water masses, with lower benthic biomass and associated Simpson dominance, an index which gives greater weight to common species and less weight to rare species (Grebmeier et al., 1989; Feder et al. 2007). Elsewhere, more organic carbon exported to the benthos often allows a smaller subset of species to dominate by biomass and reduce macrofaunal community diversity. By comparison, more diverse areas occur in nearshore sites in Alaska Coastal Water, which in the open water period has warmer, less saline, and less productive water than the colder and more saline, productive waters of the Anadyr Current to the west. These waters converge in the central Chukchi Sea north of Bering Strait to form a mixed Bering Sea water (with winter and summer water types) with resulting variability in benthic biodiversity. These water masses, which combine multiple, interacting environmental parameters, such as temperature, salinity, nutrients, and organic carbon load, have been shown to influence biodiversity (Grebmeier et al., 1989; Feder et al. 2007; Waga et al. 2020; Mueter et al. 2021).

Future changes in these environmental drivers are uncertain, although warming waters and resulting reductions in sea ice cover have been occurring for several decades (Frey et al. 2023). These trends have caused dramatic shifts in marine ecosystems as some populations of organisms have contracted northward in response to warming (Grebmeier et al., 2018) while others have expanded northward (e.g., some subarctic fishes and marine mammals, Alabia et al.,

2023). While there is clear evidence for these shifts, predicting overall biodiversity change is more difficult. It will likely be community-dependent, influenced by life history traits of specific taxa and the resulting expansion and retraction of population ranges in an ice-free Arctic (Renaud et al., 2015; Renaud et al., 2019). For sessile benthic macrofauna, range expansions are primarily limited to a larval dispersal stage, which are dependent on physical drivers like currents for transporting released larval stages of these organisms to the overlying water (Ershova et al., 2019; Renaud et al., 2015). Notably, some species bear live young without a pelagic larval stage and release directly to the benthic environment. These species, such as ampeliscid amphipods, are therefore limited in their capacity to expand home ranges in response to changing conditions.

Understanding how environmental parameters, such as reductions in sea ice and warming waters, affect benthic community composition can give insight into the potential for range expansion and contractions and gauging the resiliency of these communities to current and future warming. Biodiverse systems are often more resilient to change as there is more overlap in functional niches to fulfill ecosystem function (Solan et al., 2004). Functional niches relate to a range of biological characteristics possessed by organisms that serve particular roles in ecosystems, i.e. bioturbation and nutrient cycling. Overlap in functional niches mean that there are more than one species performing vital ecosystem functions. Sessile, long-lived benthic macrofauna also respond and are structured by overall water column processes (Grebmeier et al., 2018), so understanding changes in benthic community composition can provide insight into overall ecosystem response. Furthermore, it is important to understand benthic community composition as they are important prey for higher trophic animals (Moore et al., 2006, 2014).

2.1.2 Study Objectives

The goal of this study is to identify changes in Pacific Arctic macrofaunal biodiversity that have occurred over the last 20 years and to evaluate key drivers of that change. Time-series statistical modeling of the Shannon Index (SI) of macrofaunal biodiversity in the Distributed Biological Observatory (DBO) can provide insight into the climate impacts on the biodiversity of Arctic shelves. The SI (Shannon, 1948) has traditionally been used to summarize overall community diversity by taking into account each species' proportion to the overall ecosystem (Margalef, 1967). Additionally, it can be applied to both fine and coarse-scale taxonomic categories and genomic data (Konopiński, 2019).

This chapter focuses on statistical analysis of trends in biodiversity based on taxonomic characteristics. Records of macrofaunal benthic biodiversity in the Pacific Arctic in relation to specific environmental data, such as sediment grain size and heterogeneity, are available at the DBO time series stations since the late 1990s and can be appropriate for studying biodiversity change over time when warming or other changes have occurred in a region. Parallel measurements of environmental conditions have all occurred at these sites.

2.1.4: Hypotheses

$H1_a$: Macrofaunal biodiversity will be highest at sites with high bottom sediment heterogeneity, namely a range of sediment grain sizes as idealized in Fig. 2.1.

$H1_0$: Macrofaunal biodiversity will not change in relation to sediment heterogeneity.

$H2_a$: As seasonal sea ice persistence declines, it will negatively influence biodiversity.

$H2_0$: As seasonal sea ice persistence declines, it will not influence biodiversity.

$H3_a$: Higher bottom water temperatures will cause higher macrofaunal biodiversity.

$H3_0$: Higher bottom water temperatures will not affect macrofaunal biodiversity.

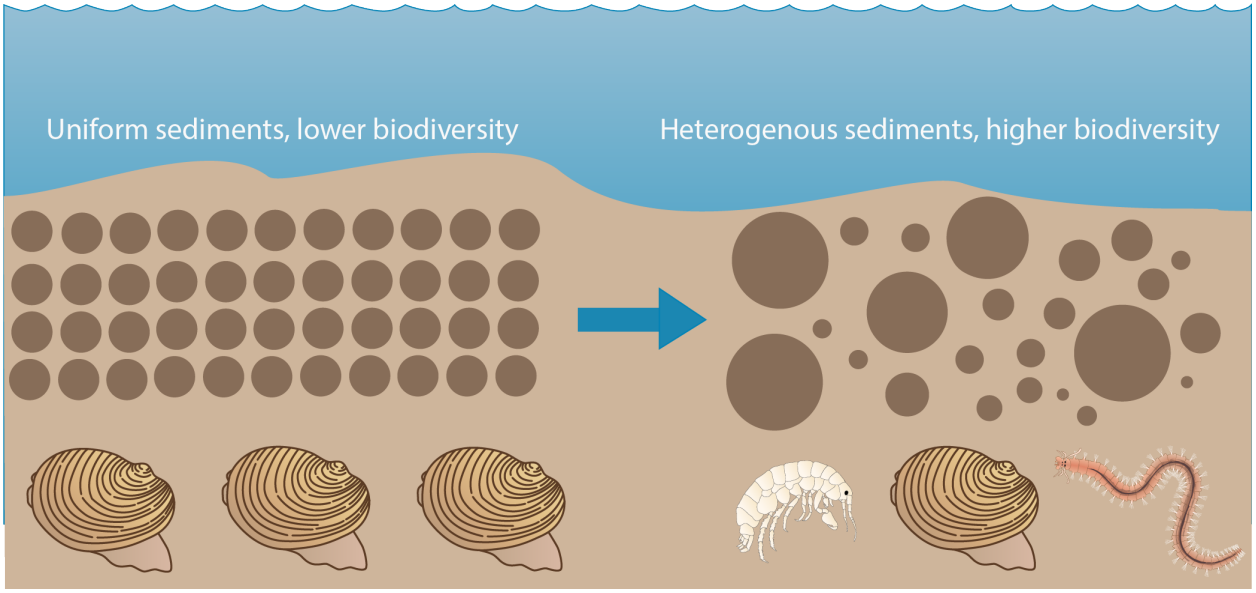


Figure 2.1. Conceptual diagram illustrating that sediment heterogeneity can be expected to positively influences biodiversity as it corresponds to increased niche space. Sediment heterogeneity is the diversity of sediment grain sizes in an area. Gravel and coarse sand are larger sediments, while mud and silt are smaller sediment grain sizes. Macrofaunal biodiversity will be highest at sites with high bottom sediment heterogeneity, represented by a larger range of sediment grain sizes. Because different animals are associated with different sediment types, higher sediment heterogeneity corresponds to increased niche space.

2.2 Materials and Methods

2.2.1 Nomenclature

When internationally coordinated sampling at DBO sites started in 2010, most of the time series stations were given standardized DBO numbered names, e.g. DBO1.1 1.2, 2.3, etc., although also retaining prior station names. Some stations that had been and continue to be

included in sampling efforts were not however given these DBO designations because they didn't lie on the standard transect lines. Some of these sites (namely the University of Tennessee (UTN)) sites represent the longest occupied time series sites. The length of these time series, as well as these sites having high benthic macrofaunal biomass, make them ecologically valuable records of change. For convenience, I have used these former historic names throughout this thesis, rather than the more recent standardized names, but provide conversions below (Table 2.1). In this study, the region is divided into DBO sub-regions 1-4; DBO1: SLIP stations, DBO2: UTBS stations, DBO3: UTN and SEC stations, and DBO 4 stations are defined as sub-regions.

Table 2.1. Historic station and current DBO stations names, latitude, longitude and length of occupation. Key: SLIP =St. Lawrence Island Polynya, UTBS=University of Tennessee Bering Strait, UTN=University of Tennessee Historical Stations, SEC=SE Chukchi Sea.

Historic Station Name	DBO Station Name	Latitude	Longitude	Estimated depth (m)	Length of Time series Occupation (years)
SLIP1	DBO1.1	62.010	-175.060	80	20
SLIP2	DBO1.2	62.050	-175.210	82	20
SLIP3	DBO1.3	62.390	-174.570	71	20
SLIP5	DBO1.6	62.560	-173.550	70	20
SLIP4	DBO1.8	63.030	-173.460	66	20
UTBS1	DBO2.5	64.992	-169.135	48	20
UTBS2	DBO2.2	64.683	-169.099	45	19
UTBS4	DBO2.4	64.959	-169.883	48	20
UTBS5	DBO2.1	64.667	-169.922	47	20
UTN2	n/a	67.051	-168.733	45	22
UTN3	n/a	67.333	-168.998	50	22
UTN4	n/a	67.501	-168.913	50	22
UTN5/SEC1	DBO3.8	67.671	-168.958	51	22
UTN6	n/a	67.736	-168.439	49	22
UTN7	n/a	67.999	-168.933	58	22
SEC8	DBO3.1	68.300	-166.935	34	7
SEC7	DBO3.2	68.242	-167.122	43	7
SEC6	DBO3.3	68.185	-167.308	48	7
SEC5	DBO3.4	68.128	-167.495	49	7
SEC4	DBO3.5	68.013	-167.867	53	9
SEC3	DBO3.6	67.898	-168.235	59	9

SEC2	DBO3.7	67.783	-168.602	50	9

2.2.2 Data Collection

2.2.2.1 Macrofaunal biodiversity

All macrofauna samples were collected within a single month annually in July from 1998 to 2019 on the Canadian Coast Guard Ship (CCGS) Sir Wilfrid Laurier. A 0.1 m^2 weighted van Veen grab was used to collect 1 to 4 replicate samples. Samples were sieved through 1-millimeter screens and preserved in 10% buffered seawater formalin. On shore, animals were identified to the lowest taxonomic level possible, counted to provide abundance data, and weighed to provide wet weight biomass.

SI was calculated at the family level for each site each year using the following formula:

$$H = -\sum_{i=1}^{s} P_i ln P_i$$

where H is the Shannon diversity index, s is the number of families and Pi is the proportion of individuals of a given family in the sample, or the number of individuals of a given family divided by the total number of individuals.

2.2.2.2 Environmental Parameters

Environmental variables compared to biodiversity were selected from a larger set of variables available and included July bottom water temperature (°C), bottom water salinity (psu), surface (0-2 cm) sediment chlorophyll (mg/m²), the surface sediment total organic nitrogen (TON, %), and total organic carbon (TOC, %). Additionally, sediments were analyzed for grain size composition. Sediments were dried at 60°C, and sorted into five sediment size classes using a Ro-tap machine (Gilson, Lewis Center, Ohio, USA): ≤0 ϕ =coarse sand and gravel, 1 ϕ -=coarse sand, 2 ϕ =medium sand, 3 ϕ =fine sand, 4 ϕ =very fine sand, and ≥5 ϕ =silt and clay. Each fraction was weighed, and percent weight for each size class was determined. A more

detailed accounting of the methods used for these environmental variables is provided further in Grebmeier et al. (2018). All sediment data refers to surface sediments (~0-2 cm). Sea ice data was collected through satellite observations following methods described in Frey et al. (2023; also K. Frey, personal communication). Average sea ice persistence (DOY=number of days of ice coverage above a 15% threshold in spatial area in a given year), and ice breakup date (day of year (DOY) when sea ice cover fell below that 15% threshold) were the sea ice parameters included in the analysis. Sea ice concentrations were estimated using the Scanning Multichannel Microwave Radiometer, Special Sensor Microwave/Imager, and/or Special Sensor Microwave Imager/Sounder passive microwave instruments carried aboard several satellite platforms, and calculated using the Goddard Bootstrap (SB2) algorithm (Comiso et al., 2017).

A sediment heterogeneity index, $\hat{p}$, was developed by calculating the variance in the percent of different sediment size classes using the following formula:

$$\hat{p} = p * (1 - p)$$

$$where\ p\ is\ the\ proportion\ of\ all\ coarser, sandier\ sediments\ ranging\ from\ 1 - 4\ \phi\ to\ all\ finer, silt\ and\ clay\ sediments \geq 5\ \phi\ at\ each\ site$$

This sediment heterogeneity index, $\hat{p}$, served as a proxy for habitat heterogeneity.

2.2.3 Regionwide Biodiversity Model Selection

A time series of SI, as well as selected environmental variables, were plotted for each sample site for all available years to visualize trends. Environmental variables tested in a mixed-effects regression analysis were selected using a Spearman's rho rank correlation analysis to determine the strength of the association between the SI and environmental parameters.

Predictor and response variables vary naturally between years and sampling locations. To examine overall trends in biodiversity independent of this natural variation, the mixed effects model was fitted with a random effects structure (Dedrick et al., 2009). Two models relating SI

to environmental predictors were fitted with restricted maximum likelihood (REML) and random effects structures organized by station alone and year and station together (Maestrini et al., 2024). Akaike Information Criteria (AIC) were then used to compare models and the model with the lower AIC value was chosen as the best random effects structure (Akaike, 1976). A variance inflation factor (VIF) with a threshold of >2.5 was used to determine collinearity between predictor variables (Fox, 2016). The colinear variable with the highest VIF was excluded from further analysis. Maximum likelihood (ML) was used to exclude insignificant variables from final models. REML was used to refit the final linear mixed-effects model describing the relationship of SI to environmental predictors (Fox, 2016). Unless otherwise indicated, statistical significance was determined using the threshold $p < 0.05$.

2.2.4 Sub-regional benthic macrofaunal biodiversity

In order to confirm region wide modeling of biodiversity, finer scale, sub-regional patterns were examined. Additionally, the length of sea ice persistence and breakup date collected at each SLIP (DBO1) and UTN station (DBO3 region) from 1998-2019 allowed for a closer examination of these variables as drivers of biodiversity. Conversely, because of limited data for the stations UTBS (DBO2), SEC (DBO3), and the DBO4 sub-regions, average sub-regional sea ice persistence and breakup dates were used. In each DBO sub-region, the SI and associated composite of environmental parameters were plotted for all available years and fitted with a centered moving average with a rolling window of 3 years (the average of the current, preceding one year, and subsequent one year) to determine trends using Student's T-tests and Mann-Kendall tests and sieve-bootstrapped versions of both of these tests (Fuertes, 2008). Model selection methods from section 2.2 were implemented to more closely examine sub-regional drivers of biodiversity and compare them with regional drivers. All statistical analyses were conducted in R version 4.3.2 (2023-10-31), released on October 31, 2023.

2.3 Results

2.3.1 Region-wide biodiversity

Regionwide, higher SI diversity was significantly correlated with July bottom water temperature and salinity, bottom surface sediment chlorophyll, the sediment grain size heterogeneity index, TOC, TON, and average sea ice persistence (Table 2.2). Some of these correlations were positive and some negative, meaning that different environmental parameters were associated with higher or lower diversity i.e. higher temperature was associated with lower diversity. For both region-wide and sub-regional model building, a random effects structure organized by station had lower AIC values than the random effects structure organized by time and station, so the random effects structure organized by station was used for all model building. For all region-wide and sub-regional analyses, surface sediment heterogeniety, total organic carbon (TOC) and totally organic nitrogen (TON) were collinear according to VIF, so in each case the variable with the lower VIF was included in further ML analyses (Table 2.3). ML analysis indicated that sediment heterogeneity, bottom water salinity, and surface sediment TON were predictive environmental parameters influencing SI. A final model linear mixed-effects model was refitted with REML and indicated that sediment heterogeneity, bottom water salinity, and surface sediment TON were predictive of SI with a random intercept assigned to station:

$$SI_{\text{station, }time} = \underset{0.10}{-3.50} + \underset{0.54}{1.78}\,_{sediment\ heterogeneity} + \underset{0.45}{1.02}\,_{TON} + \underset{0.06}{0.17}\,_{salinity} + \beta_{\text{station,time}} + \varepsilon_{\text{station, }time}$$

$$where\ \sigma_\beta = 0.52, \sigma_\varepsilon = 0.33, \beta = N\left(\mu,\ \sigma_\beta^2\right),\ \varepsilon = N\left(\mu,\ \sigma_\varepsilon^2\right)$$

Table 2.2. Spearman's rho rank correlation analysis of Shannon index (SI) diversity for all DBO stations combined, as well as DBO sub-regions (DBOs 1-4) and UTN stations in the DBO3 region. Nearshore DBO3 (SEC) refers to SEC4-8. Columns 2-3 are water parameters, 4-7 are sediment parameters, and 8-10 are ice parameters. Bolded rho values indicate statistical significance ($p < 0.05$).

Station	Bottom water temperature (°C)	Bottom water salinity (psu)	Surface sediment chlorophyll (mg/m²)	Sediment heterogeneity (index)	Total organic nitrogen (%)	Total organic carbon (%)	Average ice persistence (days)	Specific ice persistence (days)	Specific ice breakup (day of the year)
DBO (all)	**-0.27***	**-0.33***	**-0.25***	**0.36***	**-0.13***	**-0.11***	**-0.29***	n/a	n/a
DBO1 (SLIP)	0.06	-0.06	-0.18	**0.53***	**-0.33***	**-0.28***	-0.19	**-0.24***	-0.06
DBO2 (UTBS)	0.14	**0.26***	0.16	**0.38***	0.21	**0.39***	-0.2	n/a	n/a
DBO3 (UTN)	0.16	**-0.22***	**-0.21***	**0.4***	**-0.31***	**-0.32***	0.14	0	0.05
Total DBO3 (SEC)	**0.41***	**-0.47***	**-0.30***	**0.48***	**-0.55***	**-0.56***	-0.11	n/a	n/a
Nearshore DBO3 (SEC4-8)	**-0.16***	**0.15***	**-0.02***	**0.40***	**0.03***	**-0.03***	0.15	n/a	n/a
DBO4	-0.03	-0.05	-0.1	0.08	-0.06	-0.11	0.04	n/a	n/a

Table 2.3. Total organic carbon and total organic nitrogen were auto-correlated at the regional and sub-regional scale. In each case, the environmental parameter with the lower variance inflation factor (VIF) was used in further model building.

Location	Total Organic Carbon VIF	Total Organic Nitrogen VIF
Entire DBO region	2.658	2.613
DBO1	6.161	6.199
UTN	2.302	2.153
DBO3 (SEC)	17.489	16.937
Nearshore DBO3 (SEC)	9.482	8.328

2.3.2 Dominance in each DBO sub-region

Changes in dominant macrofauna can impact benthic biomass (Grebmeier et al., 2018), but abundance changes and their effect on biodiversity trends over the time period of this study are uncertain. This section summarizes trends in the most abundantly dominant macrofaunal classes at each DBO sub-region examined in this thesis. The dominant animals by abundance during the last year of this study in 2019 will also be compared to the previous times series presented in Grebmeier et al. 2018 in the following discussion section.

SLIP stations in the early 2000s were dominated by a combination of bivalves and polychaetes (Fig. 2.2). In approximately 2008, there was a shift in abundance to dominance by polychaetes in all SLIP stations and by the end of the 2010s, polychaetes were the most abundant class. The most dramatic example of this can be seen in SLIP1, SLIP2, and SLIP3. At SLIP3 from 2015-2019, where there was an increase in crustaceans and a decline in polychaetes, although polychaetes still remained the most abundant class. At the family level, in 2019 the southernmost stations (SLIP1 and 2) in the DBO1 were dominated by tellinid bivalves, followed by capitellid polychaetes (Table 2.4). SLIP4 was dominated by orbiniid polychaetes, which also were secondarily most abundant in SLIP5. The most abundant families were uristid and pontoporeid amphipods in SLIP3 and SLIP5, respectively.

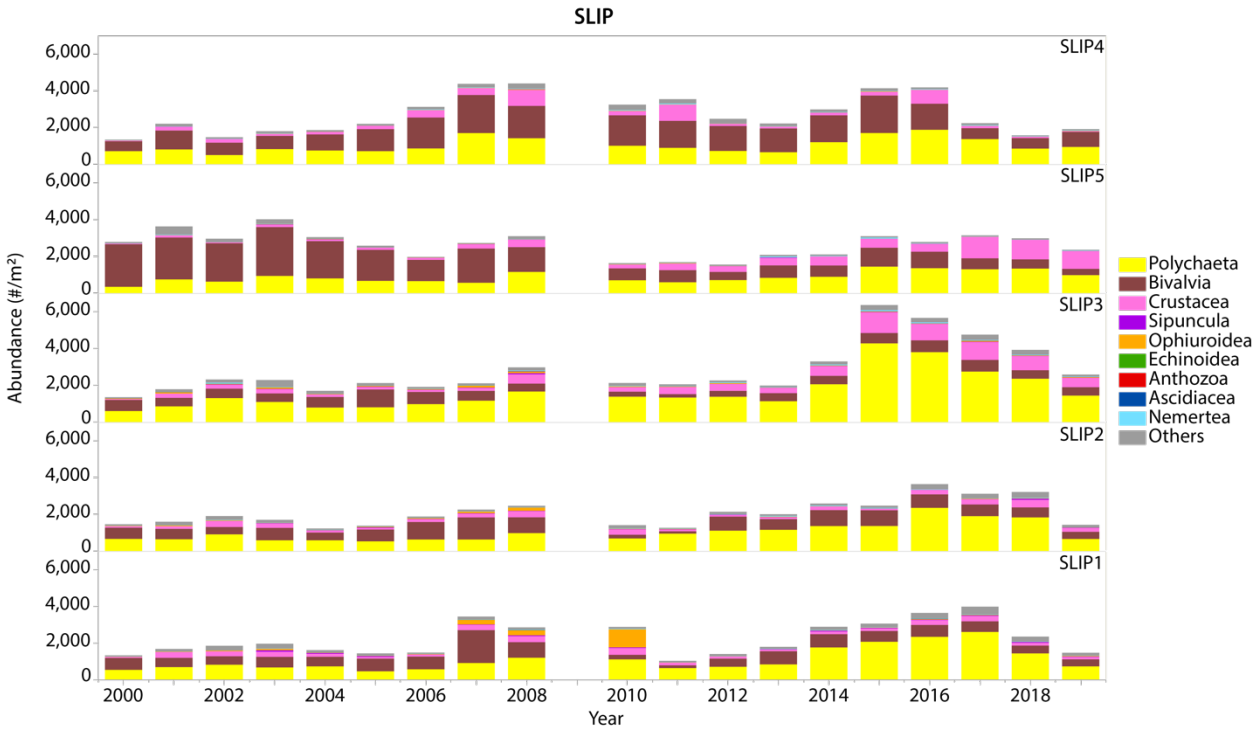


Figure 2.2. Abundance trend of dominant faunal groups at SLIP1 stations (DBO1) from 2000-2019.

Table 2.4. The top 3 most abundant macrofaunal families at each site collected in July 2019. Each family is reported as a percent abundance in relation to the total organism abundance collected at each particular site. Faunal type listed in parentheses after family names, with key: A=Amphipods, B=Bivalves, C=Cumaceans, P=Polychaetes, E=Echinoderm.

Station Name	Top 3 Most Abundant Families	Percent abundance
SLIP1	TELLINIDAE (B)	14.5
	CAPITELLIDAE (P)	10.8
	LUMBRINEREIDAE (P)	8.3
SLIP2	TELLINIDAE (B)	15.4
	CAPITELLIDAE	8.9
	NUCULIDAE (B)	7.4
SLIP3	URISTIDAE (A)	13.3
	TELLINIDAE (B)	11.7
	LUMBRINEREIDAE (P)	10.6
SLIP5	PONTOPOREIIDAE (A)	36.6
	ORBINIIDAE (P)	16.8
	NUCULIDAE (B)	8.5
SLIP4	ORBINIIDAE (P)	31.2

	TELLINIDAE (B)	20.9
	NUCULIDAE (B)	12.5
UTBS5	ISAEIDAE (A)	21.8
	CAPITELLIDAE (P)	16.2
	LEUCONIDAE (C)	12.2
UTBS2	AMPELISCIDAE (A)	32.6
	PHOXOCEPHALIDAE (A)	12.7
	ISAEIDAE (A)	10.5
UTBS1	AMPELISCIDAE (A)	35.2
	PHOXOCEPHALIDAE (A)	13.9
	ISAEIDAE (A)	11.1
UTBS4	CIRRATULIDAE (P)	13.9
	NUCULIDAE (B)	11.5
	CAPITELLIDAE (P)	8.4
UTN1	CAPITELLIDAE (P)	21.9
	TELLINIDAE (B)	16.5
	SIGALIONIDAE (P)	10.7
UTN2	TELLINIDAE (B)	28.4
	NUCULIDAE (B)	22.6
	SIGALIONIDAE (P)	12.1
UTN3	TELLINIDAE (B)	38.6
	PHOXOCEPHALIDAE (A)	23.7
	SIGALIONIDAE (P)	8.3
UTN4	TELLINIDAE (B)	44.8
	PHOXOCEPHALIDAE (A)	15.4
	SIGALIONIDAE (P)	13.4
UTN5/SEC1	PHOXOCEPHALIDAE (A)	24.7
	TELLINIDAE (B)	18
	ISAEIDAE (A)	12.8
UTN6	SIGALIONIDAE (P)	17.3
	PHOXOCEPHALIDAE (A)	11
	FLABELLIGERIDAE (P)	10.6
SEC2	OLIGOCHAETA (ANNELID)	23.1
	PONTOPOREIIDAE (A)	9.2
	PHOXOCEPHALIDAE (A)	9.1
SEC3	PONTOPOREIIDAE (A)	22.4
	SIGALIONIDAE (P)	17.7
	CAPITELLIDAE (P)	10.4
SEC4	OWENIIDAE (P)	39.2

	ECHINARACHNIIDAE (E)	18.6
	NUCULIDAE (B)	9.6
SEC5	MELITIDAE (A)	27.1
	MALDANIDAE (P)	6.5
	CIRRATULIDAE (P)	5.6
SEC6	MELITIDAE (A)	26
	CAPITELLIDAE (P)	13
	OPHIACTIDAE (E)	11.9
SEC7	CIRRATULIDAE (P)	31.9
	OPHIACTIDAE (E)	17.4
	ORBINIIDAE (P)	7.9
SEC8	OWENIIDAE (P)	73.2
	CIRRATULIDAE (P)	5.3
	SYLLIDAE (P)	3.2
DBO4.1n	DIASTYLIDAE (C)	18.1
	OSTRACODA (ARTHROPOD)	10.9
	ISAEIDAE (A)	6
DBO4.2n	CIRRATULIDAE (P)	24.4
	TELLINIDAE (B)	17.2
	NUCULIDAE (B)	9.6
DBO4.3n	CIRRATULIDAE (P)	26.4
	TELLINIDAE (B)	16.1
	NUCULIDAE (B)	9.5
DBO4.4n	TELLINIDAE (B)	23.3
	NUCULIDAE (B)	16.2
	LUMBRINEREIDAE (P)	10.5
DBO4.5n	NUCULIDAE (P)	25.2
	TELLINIDAE (B)	14.1
	LUMBRINEREIDAE (P)	13.4
DBO4.6n	CIRRATULIDAE (P)	21.5
	TELLINIDAE (B)	16.2
	NUCULIDAE (B)	11.6

The UTBS sub-region in DBO2 was dominated by Crustacea over the course of this study (Fig. 2.3). UTBS1 and UTBS2 had increases in crustacean abundance in the early 2010s. There was a potential increase in polychaete abundance occurring with a reduction in crustacean

abundance starting in 2013 through 2019. There was a reduction in crustacean abundance at UTBS4 starting in 2003 and a potential increase in polychaete relative abundance from 2016-2019. There was an increase in polychaete abundance in UTBS5. In 2019, ampeliscid amphipods were dominant at both UTBS1 and 2 to the east and isaeid amphipods at UTBS5 at the southwest station (Table 2.4). UTBS4 to the northwest was dominated by cirratulid polychaetes.

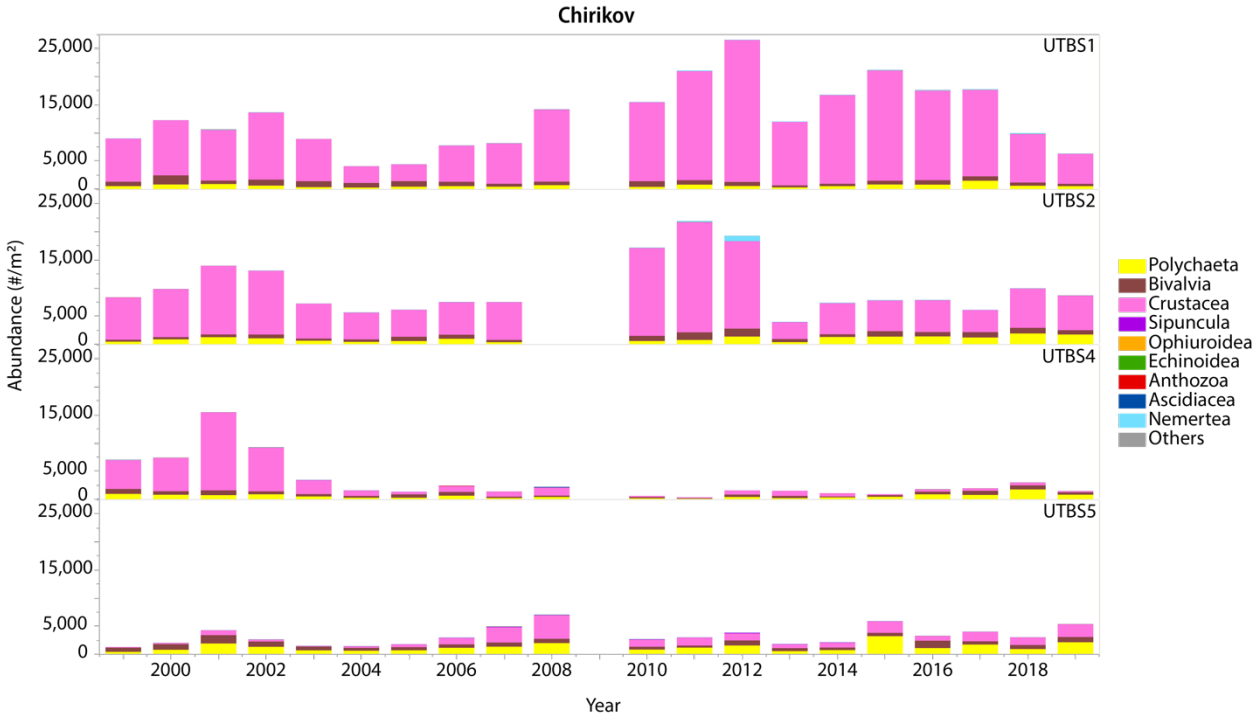


Figure 2.3. Abundance trend of dominant faunal groups at UTBS stations (DBO2) from 1999-2019.

UTN1, 2, 3, and 4 in the southcentral Chukchi Sea in the DBO3 region shifted in dominance from Crustacea to Bivalvia and, to a lesser extent, Polychaeta, starting roughly between 2008-2010 (Fig. 2.4). Specifically, in 2019, UTN1, 2, 3, and 4 were dominated by tellinid bivalves (Table 2.4). UTN5/SEC1 and UTN6 had a slight shift from Crustacea to Polychaeta, while UTN7 remained dominated by Crustacea from 1998-2019. In 2019, the northernmost part of this region, phoxocephalid amphipods and siglionid polychaetes dominate

in the more northern stations in the DBO3 region (UTN5/SEC1 and UTN6, respectively) (Table 2.4).



Figure 2.4. Abundance trend of dominant faunal groups at UTN stations (DBO3 region) from 1998-2019.

The SEC line (DBO3) starts in the northern part of the UTN region and extends towards the Alaskan coast. From 2011 to 2017, crustacean amphipods were the dominant class at the offshore sites (SEC1-3) within SEC (DBO3) (Fig. 2.5). However, their relative abundance declined in 2018-2019. In 2019, offshore stations (SEC2 and 3) were still dominated by pontoporeiid amphipods (Table 2.4). At the eastward mid-transect station (SEC4), the community was primarily composed of other groups, such as bivalves and polychaetes. There was increase in the relative abundance of polychaetes at this station in 2018 and 2019. The nearshore sites (SEC5-8) exhibited generally lower abundance levels, consisting mainly of crustaceans and polychaetes. The station closest to shore (SEC8) had an increase in the relative abundance of polychaetes from 2016-2019. In 2019, the nearshore stations were dominated by

oweniid polychaetes at SEC8 and cirratulid polychaetes at SEC7 (Table 2.4). SEC5 and 6 were dominated by melitid amphipods.

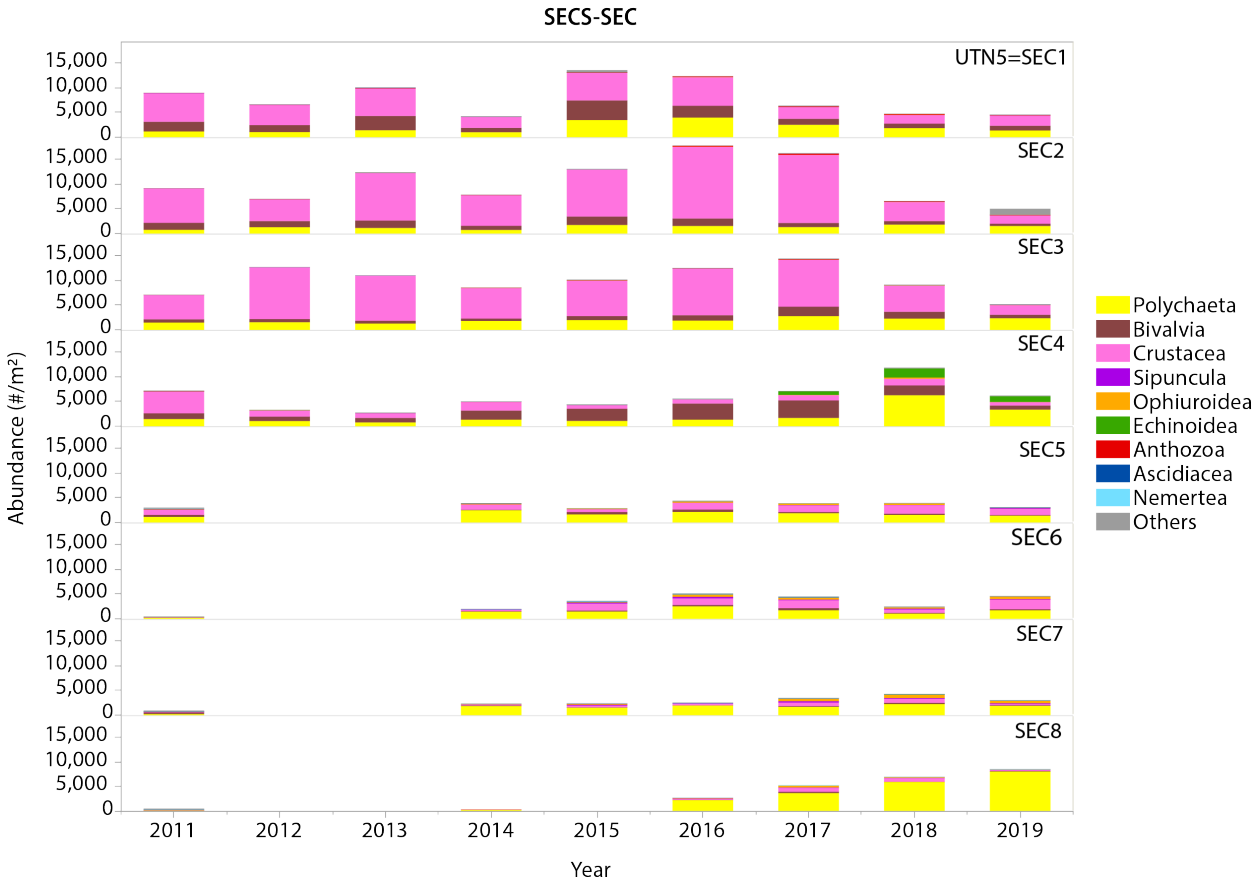


Figure 2.5. Abundance trend of dominant faunal groups at SEC stations (DBO3) from 1993-2019.

Nearshore stations in the DBO4 sub-region had a shift from Crustacea to Bivalvia and Polychaeta dominance (Fig. 2.6). A similar pattern was apparent in offshore stations DBO4.6 and DBO 4.5. DBO4.4 had a reduction in polychaetae abundance. In 2019, the station closest to shore was dominated by diastylid cumaceans (DBO4.1n) (Table 2.4). The rest of the stations were dominated by a mix of cirratulid polychaetes and tellinid and nuculid bivalves.

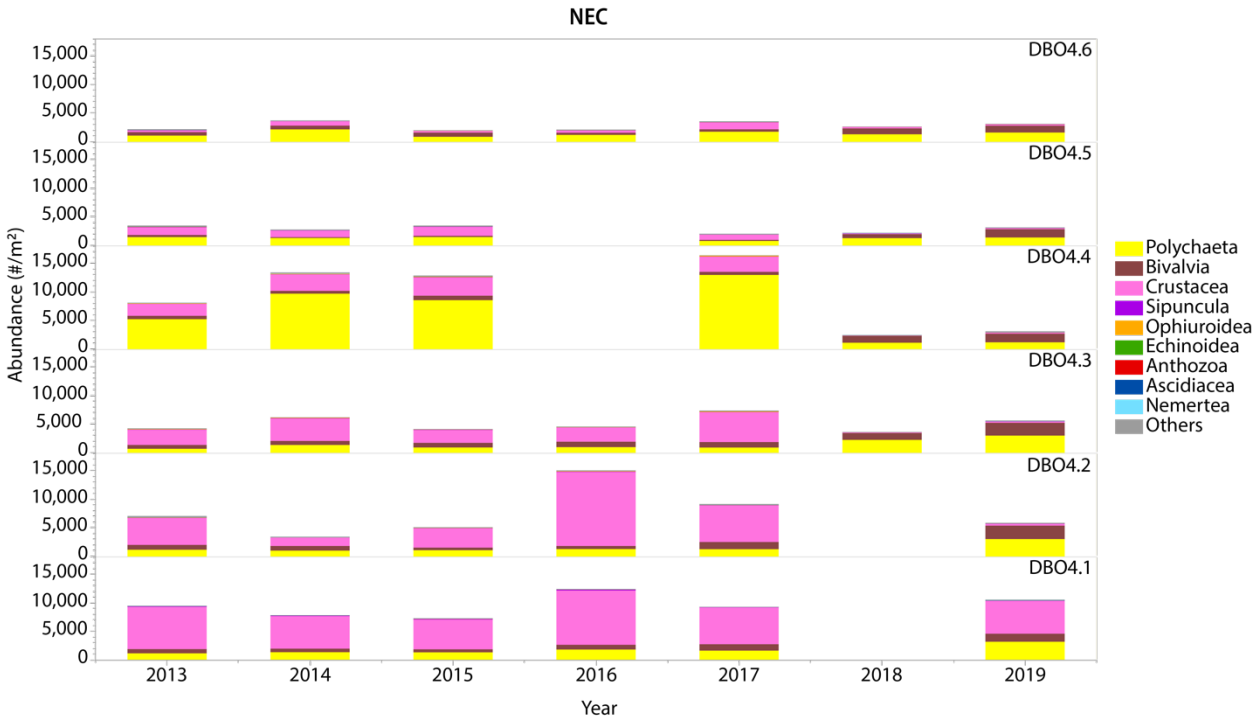


Figure 2.6. Abundance trend of dominant faunal groups at DBO4 stations from 2013-2019. Note from 2013-2017 the original DBO4 stations were located south of the new DBO4n sites that were relocated further north in 2018-2019 and likely impact the evaluation of the trend.

2.3.3 Biodiversity trends in each DBO sub-region

SLIP (DBO1)

At SLIP stations (DBO1), surface sediment heterogeneity was significantly positively correlated with SI diversity, while TOC, TON and sea ice persistence were significantly negatively correlated (Table 2.3). ML analysis found that sediment heterogeneity and sea ice persistence also influenced biodiversity over the time period. A final model was devised using REML.

$$SI_{station,\,time} = \underset{2.76}{-2.30} + \underset{0.63}{1.39}\,_{sediment\ heterogeneity} + \underset{0.00}{-0.002}\,_{Ice\ break\ up} + \beta_{station} + \varepsilon_{station,\,time}$$

$$where\ \sigma_\beta = 0.26, \sigma_\varepsilon = 0.21, \beta = N\left(\mu,\ \sigma_\beta^2\right),\ \varepsilon = N\left(\mu,\ \sigma_\varepsilon^2\right)$$

SLIP1 and SLIP5 had increasing biodiversity over the time period from 2000-2019 (Fig. 2.7). This increase in biodiversity was associated with a shift in dominance at these sites from bivalves to polychaetes over the course of the study period. At SLIP3, polychaete abundance peaked in 2017 and declined in 2018-2019. SLIP5 had an increase in crustacean abundance from 2017-2019. Surface sediment heterogeneity did not significantly change at these stations, which was found to be an important driver of biodiversity. An earlier trend in sea ice breakup day was apparent at SLIP1 and SLIP5 (Table 2.5; Fig. 2.8), which possibly influenced changes in biodiversity and community composition.

Table 2.5. Summary of time series length, Student's T-tests, Mann Kendall tests, sieve bootstrapped T-tests, and sieve-bootstrapped Mann Kendall tests for SI at SLIP, UTBS, and UTN stations. Bold type and an asterisk indicate statistical significance ($p < 0.05$).

Station	Time series length (years)	Student's T-Test	Mann-Kendall Test	Bootstrapped Student's T-test	Bootstrapped Mann-Kendall Test
DBO1.1 (SLIP1)	20	**0.46***	**0.46***	**2.49***	**0.33***
DBO1.6 (SLIP5)	20	**0.12***	**0.41***	1.05	0.28
DBO2.2 (UTBS2)	20	**0.04***	**0.61***	5.02	0.61
DBO2.4 (UTBS4)	20	**0.07***	**0.62***	5.96	0.62
DBO3 Region UTN3	22	**0.17***	**0.38***	-1.46	-0.28
DBO3 Region UTN5	22	**0.34***	**0.43***	2.05	**0.31***

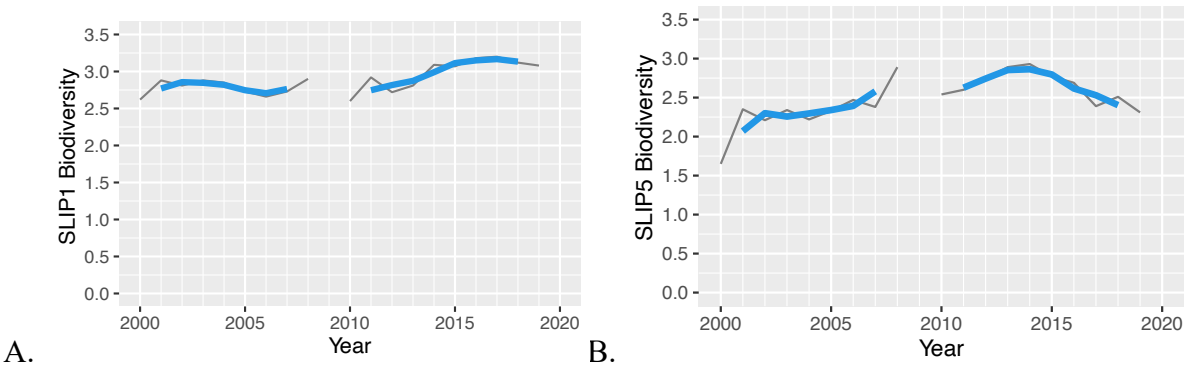


Figure 2.7. Increasing Shannon index trends in DBO1 at SLIP1(A) (Mann-Kendall tau = 0.46, $p < 0.001$) and SLIP 5 (B) (Mann-Kendall tau = 0.4, $p < 0.001$). Gray line shows data and blue line shows a moving average of 3 years to provide for trend visualization.

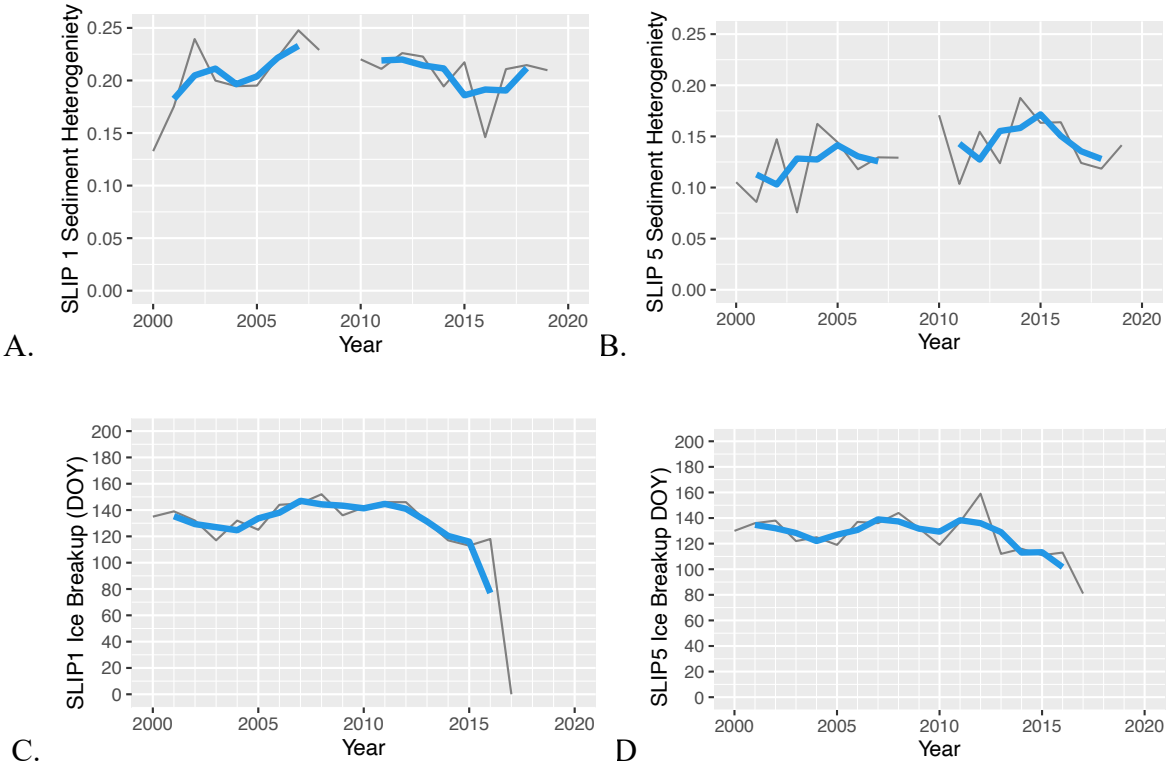


Figure 2.8. Surface sediment heterogeneity (A-B) and sea ice breakup date (C-D) trends at SLIP 1 and SLIP 5. Sea ice breakup date is defined as the day of the year (DOY) that ice fell below a 15% sea ice concentration threshold. SLIP1 had no trend in sediment heterogeneity, but a significant trend (Student's t value = -2.0097, $p < 0.05$) for an earlier ice breakup date. SLIP5 also had no trend in sediment heterogeneity, but a trend existed (Student's t value = -2.2249, $p < 0.05$) for an earlier ice breakup date. Gray line shows data with the blue line shows a moving average of 3 years to facilitate trend visualization.

UTBS (DBO2)

At UTBS stations, bottom-water salinity, sediment heterogeneity and sediment TOC were significantly positively correlated with SI (Table 2.3). ML analysis showed that longer sea ice persistence had the largest influence of the variables analyzed on biodiversity over the time period studied. A final model was refitted with REML, producing the following result:

$$SI_{station,\,time} = \underset{0.239}{3.239} + \underset{0.001}{-0.006}_{\,sea\ ice\ persistence} + \beta_{station} + \varepsilon_{station,\,time}$$

UTBS2 and UTBS4 showed increasing biodiversity over the time-period from 1999-2019 (Fig. 2.9). At both stations, sea ice persistence declined (Fig. 2.10). There were slight increases in polychaete abundance at both these sites, accompanied by decreases in crustacean abundance.

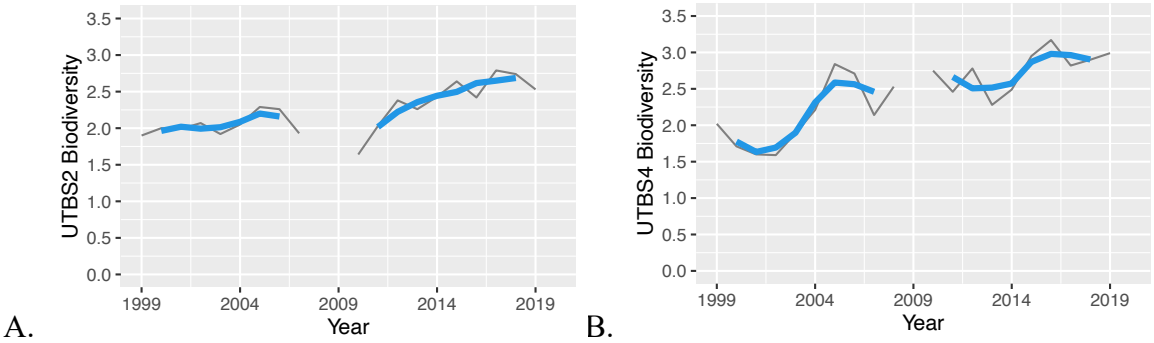


Figure 2.9. Increasing Shannon index trends at UTBS2 (A) (Mann-Kendall tau = 0.61, $p < 0.001$) and UTBS4 (B) (Mann-Kendall tau = 0.62, $p < 0.001$).

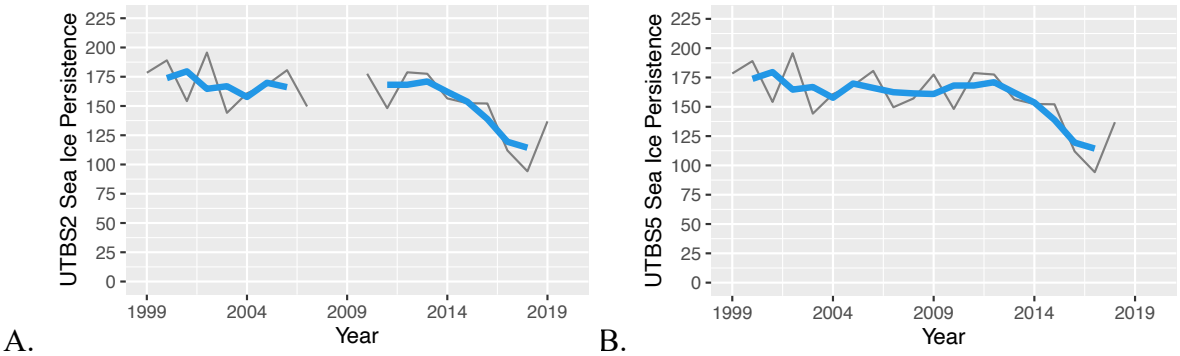


Figure 2.10. Declining trends in sea ice persistence at UTBS2 (Mann-Kendall tau = -0.446, $p < 0.001$) and UTBS4 (Mann-Kendall tau = -0.438, $p < 0.001$). Gray line show data with the blue line shows a moving average of 3 years to provide for trend visualization.

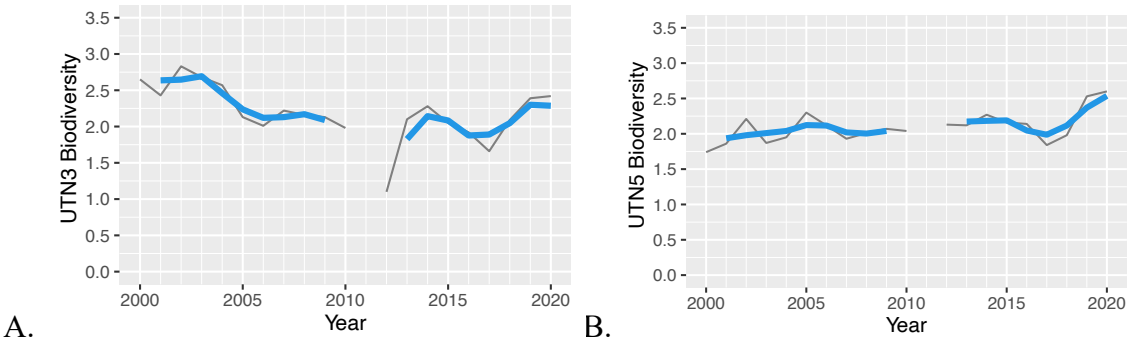
UTN (SE Chukchi Sea, DBO3 region)

At UTN stations in the DBO3 region, bottom water salinity, surface sediment chlorophyll, TOC, TON, and ice breakup day of the year were significantly negatively correlated with SI, while sediment heterogeneity was significantly positively correlated (Table 2.3). ML analysis indicated that sea ice breakup dates influenced macrofaunal biodiversity over the time period of the study. A final model was refitted with REML.

$$SI_{station,\,year} = \underset{0.399}{0.890} + \underset{0.001}{-0.004}_{\,Ice\ breakup\ day} + \beta_{station} + \varepsilon_{station,\,year}$$

$$where\ \sigma_\beta = 0.415, \sigma_\varepsilon = 0.359, \beta = N(\mu,\ \sigma_\beta^2),\ \varepsilon = N(\mu,\ \sigma_\varepsilon^2)$$

UTN3 and UTN5 had increasing biodiversity trends over the time period 1998-2019 (Fig. 2.11A, B). There was a shift in dominance from crustaceans to bivalves at UTN3 over this period. At UTN5 (also called SEC1) there was a slight increase in the relative abundance of polychaetes. At UTN3, the ice breakup had a decreasing trend, meaning that ice break up happened earlier over this time period (Fig.2.11C, Student's T-value = -0.7707, $p < 0.05$). UTN5 also had a decreasing trend for the ice breakup date (Fig.2.11D, Student's T-value = -0.93, $p < 0.05$).



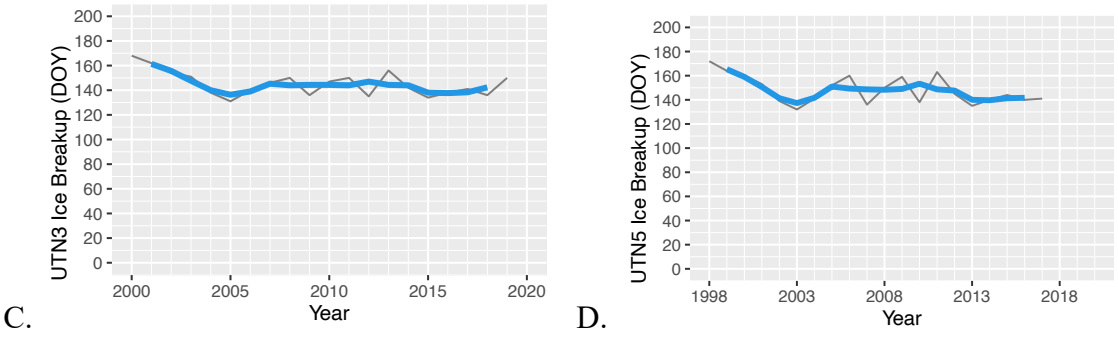


Figure 2.11. Increasing Shannon index trends at UTN3 1(A) (Mann-Kendall tau = 0.38, $p < 0.001$) and UTN5 (B) (Mann-Kendall tau = 0.43, $p < 0.001$). Sea ice breakup date is defined as the day of the year that ice falls below a 15% sea ice concentration threshold, based upon satellite observations. The gray line indicates individual station data. The thicker blue line shows a moving average of 3 years of values at stations.

DBO3 (SEC)

Bottom-water temperature and sediment heterogeneity were significantly positively correlated with SI. Surface sediment chlorophyll, bottom water salinity TOC, and TON, were significantly negatively correlated with SI (Table 2.3). ML analysis found that sediment heterogeneity had the most influence on biodiversity over the time period studied. A final model was established with REML:

$$SI_{station,\,year} = \underset{0.50}{1.33} + \underset{2.21}{5.55}\,_{sediment\ heterogeneity} + \beta_{station} + \varepsilon_{station,\,time}$$

SEC4 had decreasing biodiversity over the time period studied (Student's T-value = -0.06, $p < 0.05$) while sediment heterogeneity showed no significant trend (Fig. 2.12). SEC4 had an increase in the relative abundance of polychaetes and echinoderms in 2018 and 2019.

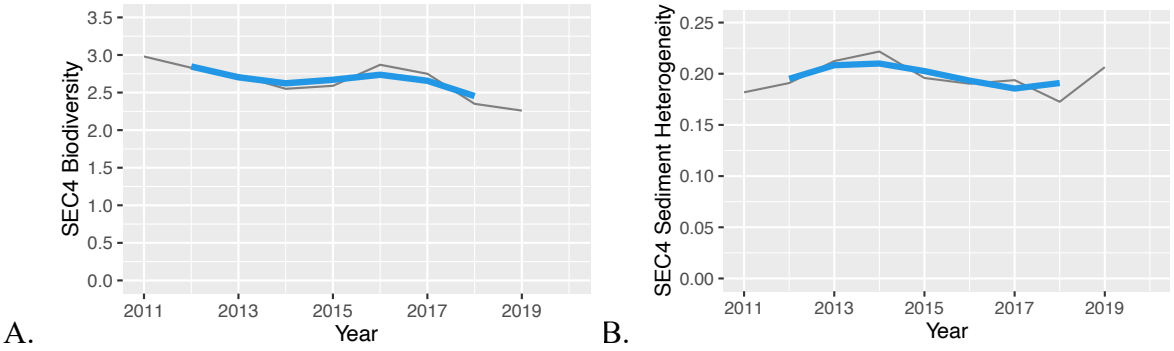


Figure 2.12. Shannon index had a decreasing trend at SEC2 (A) (Student's T-value = -0.06, $p < 0.05$) and there was no significant trend in sediment heterogeneity at the same site (B). The gray line shows data values with the blue overlaying line shows a moving average of 3 years.

SEC4 is a transitional station between the offshore (SEC1-3) and nearshore SEC stations (SEC 5-8). A Welch's t test was used to compare the mean SI of nearshore and offshore SEC stations (Welch, 1947). Nearshore SEC stations (SEC 5-8) had higher biodiversity than offshore stations (SEC1-3) (Welch's $t=7.69$, $p < 0.001$). These nearshore stations had some of the highest biodiversity in the entire DBO region, so these stations were examined separately. Summer bottom-water temperature, surface sediment chlorophyll, and TOC were significantly negatively correlated with SI. Bottom water salinity, sediment heterogeneity, and TON were significantly positively correlated with SI (Table 2.3). Bottom water temperature influenced biodiversity over the time period studied, based upon ML analysis and a final model was refitted with REML using the following formulation:

$$SI_{station,\,time} = \underset{0.251}{3.502} + \underset{0.041}{-0.134}_{\,bottom\ water\ temperature} + \beta_{station} + \varepsilon_{station,\,time}$$

There were no statistically significant trends for SI among nearshore SEC stations.

DBO4

There were no significant correlations between SI and the environmental parameters examined in DBO4 and ML analysis found no significant influences on biodiversity over the time period, so a final model was not developed.

Sub-regional comparisons

Offshore sites in SE Chukchi Sea (UTN1-6, DBO3 region) had lower biodiversity than sites in the northern Bering Sea (UTBS1-4) (Welch's $t = -5.37$, $p < 0.001$). The entire UTN sub-region had higher average sea ice persistence than the UTBS sub-region (Welch's $t = 9.14$, $p < 0.001$).

2.4 Discussion

This study confirmed shifts in community composition at many stations observed in the DBO study area. At all SLIP stations, and most dramatically at the southern SLIP stations (SLIP1-3), there was a shift in dominance between 2008-2019 from nuculanid and nuculid bivalves to capitellid and orbiniid polychaetes, which was previously observed in the southernmost portions of the region (Grebmeier et al., 2018). I observed an increase in biodiversity at SLIP1 and SLIP5, and although sediment heterogeneity was found to be an important driver of biodiversity, there was no trend over this period of study. Instead, there was a trend of declining sea ice (measured by earlier sea ice breakup) that potentially drove changes in biodiversity and community composition, likely through changes in available carbon.

At UTBS stations in the eastern Chirikov Basin, crustaceans were the most dominant class, which is consistent with previous observations (Grebmeier et al., 2018). UTBS2 and UTBS4 had increasing biodiversity at the family level from 1999-2019, also potentially driven by sea ice decline. There were slight increases in polychaete abundance, accompanied by decreases in crustacean abundance at both sites, which could have contributed to increasing biodiversity. These faunal changes could correspond to reductions in sea ice persistence and its

impact on primary production. For example, from 2010-2012 there was an increase in crustacean abundance at UTBS2, with an accompany increase in biodiversity and decline in sea ice persistence. Further study, especially at a finer taxonomic scale, could help clarify these patterns.

In the DBO3 region, UTN3 and UTN5 had increasing biodiversity over the study period, which occurred with earlier spring ice breakup. There were faunal shifts at these sites, namely from crustaceans to bivalves at UTN3 and an increase in polychaetes at UTN5. At SEC4 in the DBO region, there was a decline in biodiversity, which occurred with a decline in sediment heterogeneity. The relative abundance of polychaetes increased at this station during this time.

Accounting for variance in biodiversity through mixed-effects modelling allowed me to highlight broad, region-wide drivers of biodiversity. Mixed-effects regression modelling and trend testing through Student's T- and Mann-Kendall Tests indicated regionally positive trends of increasing biodiversity, but some negative trends in biodiversity sub-regionally. There were also trends in key environmental drivers that can impact biodiversity, namely positive trends in sediment heterogeneity, surface sediment TON, bottom water salinity, and negative trends in sea ice persistence. Examining trends in both biodiversity and environmental parameters gave insight into how biodiversity might change in the Pacific Arctic as it continues to be impacted by global warming

I hypothesized that macrofaunal biodiversity would be highest where there was a heterogeneity of bottom sediment types, meaning a variety of sediment grain sizes. Benthic taxa are typically associated with specific grain sizes (Feder et al., 1994; Feder et al. 2007). Multiple sediment types in a habitat would then increase the niche space of that habitat and support higher diversity. I found support for this hypothesis because changes in sediment heterogeneity positively influenced biodiversity, on both regional and sub-regional scales. Biodiversity across the DBO regions (DBO1-4) was primarily driven by surface sediment heterogeneity ($R^2 = 1.78$)

(Table 2.6). Surface sediment heterogeneity also drove SI sub-regionally at SLIP (DBO1) and SEC (DBO3) stations (R^2 = 1.39 and 1.68, respectively) (Table 2.6).

Table 2.6. Regional and sub-regional mixed effects models summarized. The regression coefficient (listed in parenthesis) is a measure of the strength of associated between the environmental influence and biodiversity. Sediment heterogeneity (the proportion of fine sediments to coarse sediments) corresponds to diversity of sediments and niches for benthic infauna.

Location	Environmental influences on Shannon index (regression coefficient)
DBO (ALL)	Sediment heterogeneity (1.78), sediment total organic nitrogen (1.02), bottom water salinity (0.17)
DBO1 (SLIP)	Sediment Heterogeneity (1.39), sea ice persistence (-0.002)
DBO2 (UTBS)	Sea ice persistence (-0.006)
DBO3 (UTN)	Sea ice persistence (-0.004)
DBO3 (SEC)	Sediment heterogeneity (5.55)
DBO4	No observed correlations

Other studies have shown that sediment heterogeneity influences benthic macrofaunal biodiversity in the Pacific Arctic (Grebmeier et al., 1989; Feder et al., 1994). Grebmeier et al. (1989) found that offshore locations in the SE Chukchi Sea with more heterogeneous mixtures of silt, clay, and sandy sediments have higher biodiversity than the predominately uniform sandy sediments of the northern Bering Sea, based upon taxonomic analyses in the early 1980s. I observed lower biodiversity in the 2000-2019 period, potentially driven by change in the sediment grain size and heterogeneity, which might be influenced by changing flow regimes (Woodgate, 2018). Biodiversity at offshore locations in the SE Chukchi Sea (UTN1-6, DBO3 region) was lower than biodiversity in the northern Bering Sea (UTBS1-4), and is potentially driven by changes in sediment heterogeneity at each site, i.e. a shift to more homogenous sediments in the DBO3 region and a shift to more heterogenous sediments in the UTBS region. While Spearman's rho analyses indicated that sediment heterogeneity was positively correlated

with SI at both locations, neither was found to be a primary driver following mixed-effects modelling.

By comparison, SLIP stations south of St. Lawrence Island (SLI) in the northern Bering Sea, UTBS stations north of SLI in the northern Bering Sea, and UTN stations in the SE Chukchi Sea had declining sea ice (as defined by breakup date at SLIP and UTN stations and annual sea ice persistence at UTBS stations) that was found to increase biodiversity at both locations over the time period studied. I accepted my second hypothesis that the longer presence of sea ice was associated with lower biodiversity. Average sea ice persistence was higher at UTN stations than at UTBS stations. Mixed-effects models for SLIP, UTBS, and UTN sub-regions indicated that the presence of sea ice (whether measured as persistence or breakup date) had a negative influence on biodiversity, i.e. more ice cover was associated with lower biodiversity. One possible explanation is that a longer open water period associated with less sea ice could lead to an increased food supply over a longer productive season. Furthermore, as sea ice continues to decline in the region, this increase in primary production could become a greater influence on benthic biodiversity. While the presence of sea ice was not a regionwide influence on biodiversity, it is possible that declining sea ice will ultimately result in higher productivity. Higher production with less sea ice could affect patterns of consumption in the water column, i.e. higher grazing and less carbon export to the benthos. More production related to greater open water periods could lead to more grazing. The net result of this interaction would be less immediately labile organic carbon being delivered to the benthos, resulting in lower biomass and higher biodiversity. This scenario is supported by the observation that high levels of organic carbon exported to the benthos are utilized by a few dominant species that have high benthic biomass (Grebmeier et al., 1989). So, based upon this reasoning, if ice cover at the UTN stations persists longer than at other studied locations, biodiversity could decline. The southernmost UTN

stations are experiencing greater sea ice loss than more northern stations, so effects on biodiversity are likely latitudinally dependent.

For all the DBO regions studied (1-4), I did not accept my third hypothesis that an increase in bottom water temperature has a positive influence upon macrofaunal biodiversity. Another study in the northeast Chukchi Sea found site-specific macrofaunal benthic species richness was lower during a year of higher water temperatures but found no significant difference in overall macrofaunal community diversity, i.e. Shannon diversity (Mueter et al., 2021). Higher July water temperature was found to be a negative influence on biodiversity at nearshore sites in the southeast Chukchi Sea. Since these nearshore stations are some of the most biodiverse sites in the study region, further study is warranted to establish more clearly the connections between bottom water temperatures and biodiversity.

Regionwide, higher salinity and TON positively influenced biodiversity. These two environmental paraments are associated with different water masses in the region. Different water masses in the Pacific Arctic have long been thought to drive benthic community structure (Feder et al., 1994; Feder et al., 2007; Grebmeier et al., 1989; Grebmeier et al., 2006; Sirenko and Gagaev, 2007; Waga et al., 2020). Typically, high nutrients in more saline water is generally associated with higher biomass and lower overall diversity.

Regionally and at individual stations, I found that surface sediment heterogeneity had a positive influence on biodiversity. The specific relationships of organismal diversity to variable grain size classes should be further explored, as there is a limited understanding of how sediment size class structure could be affected by warming. For example, currents speeds have increased regionally (Woodgate et al., 2018), which likely will influence the compositions of sediment size classes. This increased water flow is possibly changing the distribution of sediment size particle classes, and thus altering patterns of biodiversity.

Additionally, I found that biodiversity at some stations was negatively influenced by the length of sea ice persistence and later break up dates. As sea ice declines in the region, this change, which appears to increase biodiversity and subsequent ecosystem resiliency, could become more widespread.

Both functional redundancy and biodiversity support ecosystem stability and resilience in the face of change (Hewitt et al., 2008; Iken et al., 2020). Resilient ecosystems are able to maintain ecosystem function through disturbances that might otherwise lead to extirpation of specific taxa. This resiliency is accomplished through functional redundancy in which biological traits that accomplish important ecosystem functions, i.e. nutrient cycling, occur simultaneously across multiple taxa. Resiliency is also by extension accomplished through greater biodiversity, which provides a wider breadth of functional biological traits that can be utilized in response to disturbance.

Currently, the length of sea ice persistence per year is a weak, but negative driver of biodiversity. Although it is not a driver over the entire region, there is a relationship between biodiversity and sea ice duration. As sea ice persistence decreases, its influence on biodiversity could become more pronounced and region wide. Sea ice persistence directly influences seasonal phytoplankton production and export of organic carbon to the benthos. Generally, higher carbon export to the benthos would lead to less biodiversity, but higher carbon export does not appear to currently be influencing biodiversity. The export of increased carbon production to the benthos could be regulated, in part, by water column grazing. With these changes, I project that benthic communities may become more biodiverse, but with lower abundances and biomass. TON and TOC were widely observed to be autocorrelated across the study region, suggestion that these two environmental parameters are linked. Continued time series monitoring and sampling would be an effective means to reveal continued changes in macrofaunal biodiversity as sea ice

continues to decline. Such continued monitoring will also aid in understanding changes in patterns of carbon cycling, as well as novel organism interactions as communities change compositionally.

Chapter 3. Pan-Arctic regional intraspecific genetic differences of three benthic macrofauna: *Ennucula tenuis*, *Macoma calcarea*, and *Cistenides hyperborea*

Abstract

A phylogeographic analysis of three benthic macrofauna from the northern Bering and Chukchi Seas was undertaken using cytochrome c oxidase (CO1) barcode data. Analysis was conducted on two clams, *Ennucula tenuis* (Montagu, 1908) and *Macoma calcarea* (Gmelin, 1791), and a polychaete, *Cistenides hyperborea* (Malmgren, 1866). These analyses were used to gain insight into the underlying drivers of population-level genetic connectivity in the seasonally productive, shallow shelves of the northern Bering and Chukchi Seas. Genetic barcode data was then compared with sequences from prior work undertaken with the same species in other parts of the Arctic to better understand the wider population dynamics of these widespread species. *Ennucula tenuis* specimens analyzed belonged to one population, with mild geographic structure. *M. calcarea* analysis was impacted by contamination and conclusions were not made about *M. calcarea* population structure. Specimens of *C. hyperborea* analyzed from the northern Bering and Chukchi Seas belonged to one population with two closely related haplotypes and almost no geographically based genetic differentiation. Sequences of the polychaete obtained during this study differed considerably from most *Cistenides* spp. specimens in the National Center for Biotechnology, indicating that there may be a discrepancy in the taxonomic identifications made during this or prior studies.

3.1 Introduction

3.1.1 Background and rationale

The Bering and Chukchi shelves contain high biomass communities of benthic macrofauna, dominated by bivalves, amphipods, and polychaetes (Grebmeier et al., 2015). In these high biomass benthic areas, a small number of species tend to dominate, which results in relatively low benthic biodiversity, but the ecosystem nevertheless supports important populations of benthivores such as walruses, eiders and gray whales (Grebmeier et al., 2015; Moore et al., 2014). This high biomass is supported, in part, by regional currents flowing through the Bering Strait region that carry nutrients that facilitate algal production and carbon export to the benthos (Coachman et al., 1975). These northward flowing currents also provide a mechanism for transport of plankton from the Pacific to the Arctic Ocean. This gateway has been an important vector for the dispersal of northern Pacific organisms into the Arctic (Layton et al., 2014; Carr et al., 2011). Benthic organisms disperse in several ways, including reproducing as planktonic larvae that spend varying amounts of time in the water column depending on their feeding abilities, egg yolk reserves, or development capabilities (planktonic, lecithotrophic, or direct development). Larvae that feed during the planktonic stage can also spend more time in the water column, increasing the dispersal distance of the organism.

The bivalves *Ennucula tenuis* (Montagu, 1908) and *Macoma calcarea* (Gmelin, 1791), and the polychaete *Cistenides hyperborea* (Malmgren, 1866) are important benthic macrofauna in the Pacific Arctic shelves with typically high abundances (Blanchard et al., 2013; Grebmeier et al., 2015; Goethel et al., 2019). Additionally, they have cosmopolitan distributions throughout much of the Northern Hemisphere (Coan et al., 2000). *Macoma calcarea* is an important prey source for walruses in the Pacific Arctic. It can deposit and filter feed, it produces pelagic larvae, and it is widely distributed in the Pacific, Atlantic and shelf areas of the Arctic Ocean (Coan et

al., 2000). *Cistenides hyperborea* is a polychaete with a planktonic larval stage and a similarly broad distribution range. Understanding the population genetics of these organisms could give insights into current ecosystem biodiversity and function, as well as the connectivity of benthic habitats in the Pacific Arctic and across the shelves of the Arctic Ocean.

Population genetics is a useful tool for understanding the dynamics of organisms in an ecosystem. In particular, it can highlight connectivity related to environmental parameters (Galaska et al., 2017). In benthic habitats in the Distributed Biological Observatory (DBO) region, sediment grain size plays an important role in the diversity of organisms (Grebmeier et al., 1989; Feder et al., 1994; Waga et al., 2020). Benthic organisms adapt to different sediment grain size composition in order to exploit different niches. The diversity of sediment grain sizes, namely the degree of heterogeneity of grain sizes, was shown to be an important factor influencing interspecific biodiversity in the DBO region (Chapter 2). It is possible that these patterns also influence patterns of divergence within species as well. Wide-scale patterns of variable regional currents influence sediment grain size (Pisavera et al., 2015), and additionally influence water column characteristics such as nutrient content and temperature (Hansell et al., 1993). Currents also play a large role in dispersal for benthic organisms, which could further impact patterns of population connectivity or divergence. Populations isolated from major currents might experience genetic drift, while populations living near major currents might display homogeneity over long distances. Additionally, population genetics can clarify estimates of biodiversity to expose species complexes or to provide evidence for the synonymization of species, i.e. combing two species (Carr et al., 2011).

3.1.2 Study area

The DBO is an existing network of time-series sampling sites for macrofaunal collections and environmental data, located at productive sites on the northern Bering and Chukchi shelves.

These sites have been sampled consistently since 2000 with the objective of recording biological and environmental change. A more detailed description of the DBO study area has been provided elsewhere (Fig. 1.1: Section 1.7). Adding genetic analysis to these benthic macrofaunal time series data adds value to the taxonomic analyses that have been already accomplished. As an explanatory note, throughout this study, sub-regionally refers to each DBO sub-region, i.e. DBO1, which consists of long-occupied stations that are referred to in some prior publications as SLIP1-5. Other DBO sub-regions are DBO2, DBO3, DBO4, and DBO5, which in the context of this thesis, are sub-regions of the DBO study area in the northern Bering and Chukchi Seas.

3.1.3 Study Objectives

I conducted a phylogeographic analysis using cytochrome c oxidase I (CO1) barcode analysis of *E. tenuis, M. calcarea,* and *C. hyperborea* across the DBO study area in order to better understand the underlying drivers of genomic connectivity across different populations. CO1 data for these species are also available from the National Center for Biotechnology Information (NCBI), enabling comparisons with other Arctic regions.

3.1.4 Hypothesis

$H1_a$: DNA barcoding will detect intraspecific diversity not apparent from morphological taxonomy for 3 macrofaunal species: the bivalves, *Ennucula tenuis* and *Macoma calcarea*, and the polychaete, *Cistenides hyperborea.*

$H1_0$: DNA barcodes will detect no intraspecific diversity.

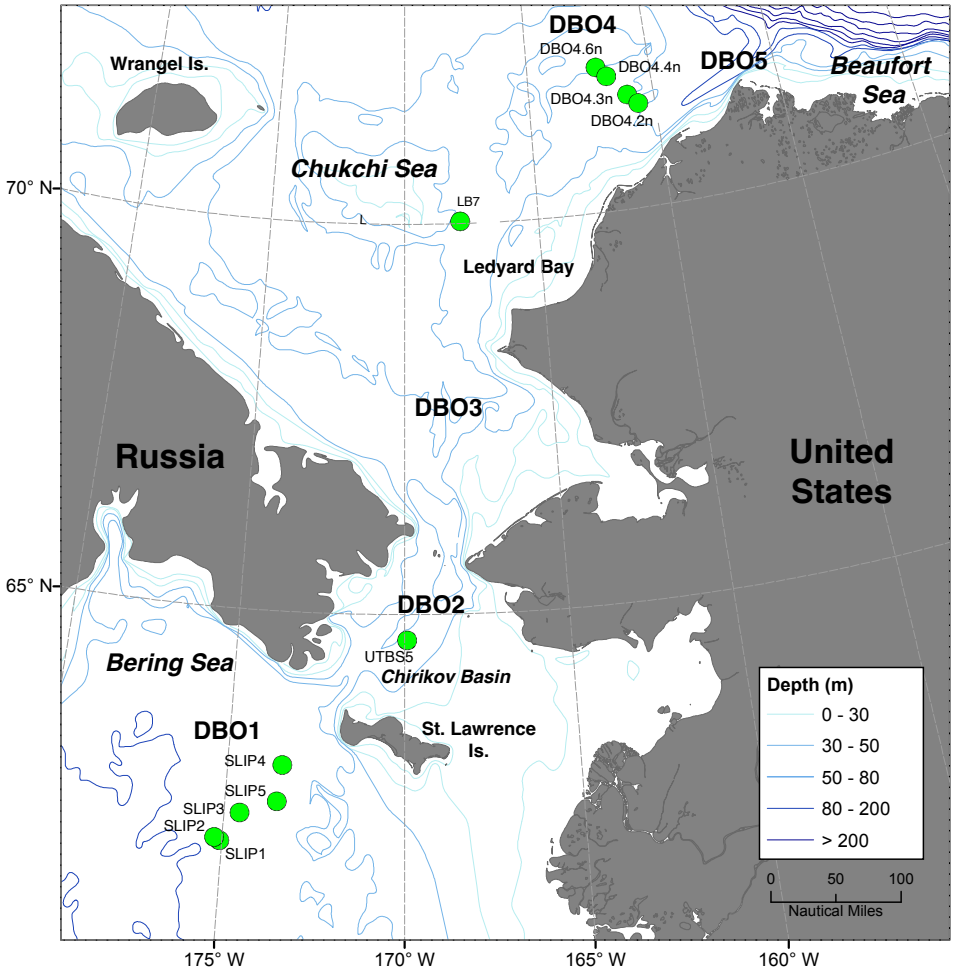
3.2 Materials and Methods

3.2.1 Data Collection

Samples of benthic macrofauna were collected using a 0.1 m^2 weighted Van Veen grab on the Canadian Coast Guard Ship Sir Wilfrid Laurier (SWL23) from July 7-27, 2023, and on the Research Vessel Sikuliaq (SKQ23) from September 10-October 4, 2023 (Fig. 3.1). Samples were sieved through 1-mm screens, identified to species shipboard, and preserved in 95% ethanol. The ethanol was changed after 24 hours to adjust for dilution. For population genetic analysis, >5 individual specimens for each species were collected and identified at each station. Species identifications were confirmed once preserved samples were returned from sea (S. Soques and A. Clarke, CBL/UMCES, personal communication). A full list of samples collected and associated collection data, is provided in the Supplementary file: S2_Silverson_popgen2023.csv. All samples are stored at the Chesapeake Biological Laboratory for further analysis.

A.





B.

Figure 3.1. A. A map of collection locations of *Ennucula tenuis, Macoma calcarea*, and *Cistenides hyperborea* specimens analyzed for population genetics, including sources of CO1 data obtained from the National Center for Biotechnology Institute (NCBI). Major sub-regions include the north Pacific, the northern Bering and Chukchi Sea combined, the Beaufort Sea, and the Hudson Bay, the North Sea, and the White Sea. B. Green circles indicate collection locations

for specimens in this study. Station IDs: DBO=Distributed Biological Observatory, SLIP=St. Lawrence Island Polynya, UTBS=University of TN Bering Sea, and LB=Ledyard Bay

3.2.2 DNA Extraction and Qubit Analysis

In total, 48 *E. tenuis*, 14 *C. hyperborea*, and 42 *M. calcarea* samples collected in 2023 from DBO sites were selected for the population genetic analysis (Appendix Table A1). A Qiagen DNeasy Blood and Tissue Kit (Qiagen, Hilden, Germany) was used to extract DNA following the manufacturer's guidance. The DNA yield of all extractions was ascertained using a Qubit 4 Fluorometer (ThermoFisher Scientific, Waltham, Massachusetts, USA) following the manufacturer's protocol to ensure an adequate DNA yield for subsequent assays.

3.2.3 PCR Preparation

A 660-base pair (bp) fragment of COI was amplified using a polymerase chain reaction (PCR) with the primers LCO1490 (5-GGTCAACAAATCATAAAGATATTGG-3) and HCO2198 (5-TAAACTTCAGGGTGACCAAAAAATCA-3) (Folmer et al., 1994). The PCR reaction was prepared with 12.5 µL 5 High-Fidelity 2x Mastermix (New England Biolabs, Ipswich, Massachusetts, USA), 1.25 µL forward primer LCO1490, 1.25 µL reverse primer HCO2198, 8 µL Nuclease-Free Water, and 2 µL DNA extract. All samples were amplified on a thermocycler with the following cycling conditions. Stage 1 comprised 1 cycle at 94°C for 3 minutes. Stage 2 comprised 40 cycles at 94°C for 30 seconds, 1 minute at 51°C, and 1 minute at 72°C. Stage 3 comprised 1 cycle at 72°C for 2 minutes. For PCR amplifications that were judged to have failed, a second protocol was used with a lower annealing temperature. Stage 1 comprised of 1 cycle at 94°C for 2 minutes. Stage 2 comprised 10 cycles of 40 seconds at 94°C, 1 minute at 45°C, and 1 minute at 72°C. Stage 3 comprised 30 cycles of 40 seconds at 94°C, 1 minute at 50°C, and 1 minute at 72°C. Stage 4 comprised 1 cycle of 3 minutes at 72°C. A 1x

TAE gel was used to check for amplification using a UVP GelStudio DNA Gel Documentation Imaging System (Analytik Jena, Jena, Germany).

3.2.4 DNA Purification, QC, and Sequencing

The remaining 23 µL PCR products were loaded and run on a large gel with 3 µL dye and a Thermo Scientific Gene Ruler 100 bp ladder was used to assess PCR product size. Bands were then cut under UV light and centrifuged for 60 seconds at 12,000 g with 40 µL AE. Samples were then frozen at -80°C for a minimum of 15 minutes, followed by centrifugation for 30 minutes. Supernatant was then stored on a PCR plate.

Gel was excised at the 660 bp region, transferred to a pre-weighed 1.5 mL tube, and weighed to obtain the weight of gel. Four times the amount of gel dissolving buffer was added, and each sample was incubated at 50°C for 10 minutes. The sample was then transferred to a spin column loaded into a collection tube and centrifuged for 1 minute at 16,000 x gravity. Supernatant was discarded and 200 µL DNA wash buffer was added to the column and centrifuged for 1 minute at 16,000 x gravity. The purified PCR products were sequenced using the Sanger et. al. (1977) method by Azenta Life Sciences (South Plainfield, New Jersey, USA).

3.2.5 Bioinformatic Analysis

Sanger sequences from Azenta Life Sciences were assembled and aligned using Geneious Prime software (vers. 2024.0.2; GraphPad Software, LLC, Boston, Massachusetts, USA) via MUSCLE (Edgar, 2004). Nucleotide assignments were checked against reference sequences from NCBI using the sample chromatogram. Final alignments and single nucleotide polymorphism (SNPs) for each of the 3 species analyzed were confirmed with MEGA software (vers. 11; Tamura et al., 2021). In MEGA, sequences were analyzed for pairwise genetic distances (F_{ST}), to recover the genetic variance between localities. Arlequin software was used to

perform an Analysis of Molecular Variance (AMOVA) (vers. 3.5.2.2, Excoffier and Lischer, 2010). All statistical analyses were performed twice; once using sequences from this study and once using sequences from this study along with all available CO1 sequences obtained from the NCBI. In the AMOVA analysis with DBO and NCBI sequences, a hierarchical level was included for the entirety of the DBO region, i.e. northern Bering and Chukchi Seas combined. Median-joining haplotype network analyses were performed using POPART software (vers. 3; Leigh and Bryant, 2015; Bandelt et al., 1999) and sequences from this study and the NCBI (Appendix Table A1). When applicable, geographic distance (kilometers) was tested as a covariable with genetic distance (pairwise F_{st}) to visualize potential isolation by distance patterns in macrofauna. A Mantel test was performed to test for this correlation (Legendre and Legendre, 2012).

3.3 Results

3.3.1 *Ennucula tenuis*

E. tenuis specimens analyzed had 30 unique haplotypes, with 20 of those occurring within the DBO region. Tajima's D, which tests for non-random selection as opposed to neutral evolution through genetic drift, was negative, which suggested the gene is most likely not evolving neutrally and the population has recently expanded (Tajima's D = -2.09, Table 3.1) (Tajima, 1989). AMOVA results showed that 87.606% of diversity occurred within localities as opposed to among localities (14.619%) or regions (-1.225%) (Table 3.2). Pairwise distance (F_{st}) indicate that the detected between-region diversity resulted from population differences in specimens from the St. Lawrence Island Polynya (SLIP) and Ledyard Bay (LB) (F_{st} = 0.22, $p < 0.05$; Table 3.3). The CO1 median-joining haplotype network for *E. tenuis* showed multiple groups of specimens (Figure 3.2).

Table 3.1. Standard nucleotide indices from *Ennucula tenuis* CO1 barcode data.

Number of samples	37
Nucleotide diversity	0.006
Segregating sites	17
Parsimony- informative sites	10
Tajima's D	-0.209
Pairwise-distance	0.01

Table 3.2. Analysis of molecular variance statistics for *Ennucula tenuis* based on CO1 data.

Source of variation	**Sum of squares**	**Variance components**	**Percentage variation**
Among seas	3.939	-0.024	-1.225
Among localities within region	6.937	0.291	14.619
Within locality	49.972	1.723	86.606
Total	60.848	1.989	

Table 3. 3. Pairwise distance (Fst) *Ennucula tenuis* CO1 data between sub-regions.

	SLIP	DBO4	UTBS	LB
SLIP	0			
DBO4	0.071	0		
UTBS	0.0541	-0.050	0	
LB	0.220	0.343	0.196	0

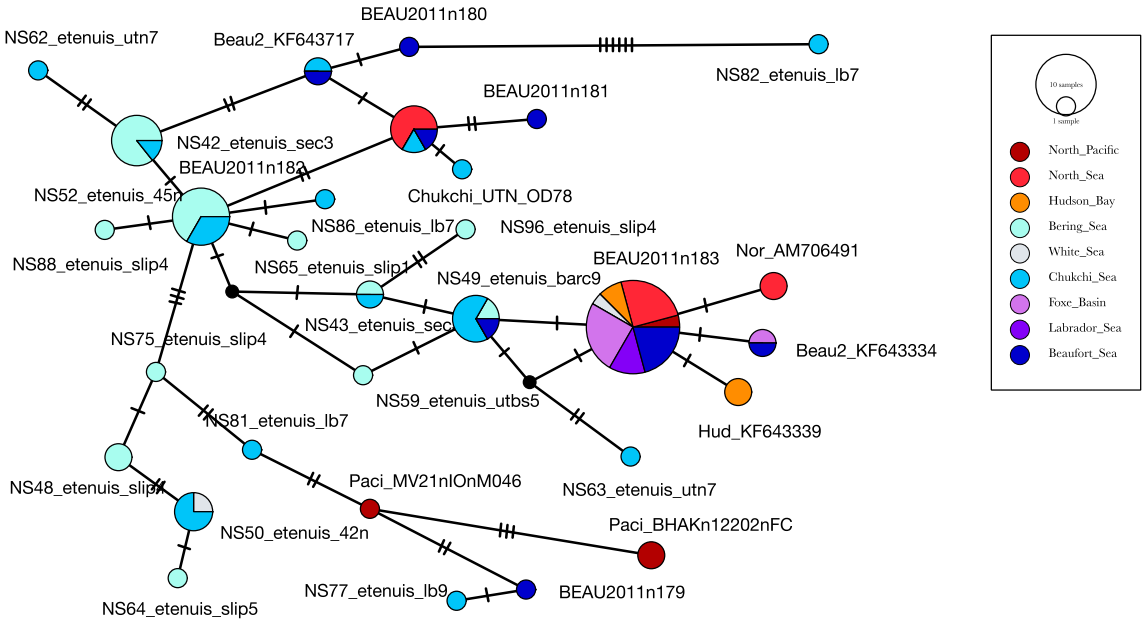


Figure 3. 2. Median-joining haplotype network based upon CO1 sequences for *Ennucula tenuis*. The size of circle represents how many specimens fit into each particular haplotype. Haplotypes are colored by location. Notches between haplotypes represent one single nucleotide polymorphism.

When comparing to other regions (Fig. 3.1A), Layton et al. (2014) analyzed *E. tenuis* CO1 sequences from the Canadian Arctic and those clams appeared to be genetically distinct from *E. tenuis* collected for this study, and especially distinct from the further south sites, e.g. SLIP stations in the northern Bering Sea (Figure 3.1B). When sequences from Layton et al. (2014) and *E. tenuis* collected from the current study were included in an AMOVA, the statistical variation differences between seas (northern Bering and Chukchi Sea combined, Beaufort, and the Hudson Bay) increased from -1.23 to 35.37% (Table 3.5). However, within locality variance still was higher, explaining 53.88% of the variance. Pairwise AMOVA showed that populations from western, central, and eastern Canada (Beaufort Sea, Iglookik, Foxe Basin, and Hudson Bay; Fig.

3.1A) were significantly different from populations from the northern Bering Sea (SLIP, UTBS) and northeastern Chukchi Sea shelf (LB; Figure 3.1B, Table 3.6,). Furthermore, populations from SLIP and UTBS were significantly different than populations from LB (the more northern site) according to this analysis.

Table 3.4. Standard nucleotide indices from CO1 barcode data for *Ennucula tenuis* from this study and across the Arctic.

Number of samples	83
Nucleotide diversity	0.009
Segregating sites	36
Parsimony- informative sites	20
Tajima's D	-1.03
Pairwise-distance	0.01

Table 3.5. Analysis of molecular variance statistics for *Ennucula tenuis* based on CO1 data from this study and other data available from across the Arctic.

Source of variation	Sum of squares	Variance Components	Percentage Variation
Among regions	27.287	0.786	41.177
Among localities within regions	7.059	0.207	10.839
Within locality	39.374	0.916	47.984
Total	73.720	1.908	

Table 3.6. Pairwise distance (Fst) between sub-regions based on *Ennucula tenuis* CO1 data from this study and studies across the north Pacific, Arctic, and North Sea.

	North Pacific	Alaska: DBO1	Alaska: DBO2	Alaska: DBO3	Alaska: Ledyard Bay	Alaska: DBO4	Canada: east Beaufort Sea	Canada: west Beaufort Sea	Canada: Igloolik	Canada: Hudson Bay
Alaska: DBO1	0.015	-								
Alaska: DBO2	0.016	0.004	-							
Alaska: DBO3	0.017	0.008	0.006	-						
Alaska: Ledyard Bay	0.016	0.012	0.012	0.015	-					
Alaska: DBO4	0.016	0.007	0.005	0.008	0.013	-				
Canada: eastern Beaufort Sea	0.014	0.011	0.010	0.011	0.014	0.011	-			

Canada: western Beaufort Sea	0.016	0.009	0.007	0.008	0.017	0.008	0.010	-		
Canada: Igloolik, Foxe Basin	0.016	0.010	0.007	0.008	0.017	0.007	0.010	0.002	-	
Canada: Hudson Bay	0.015	0.010	0.008	0.008	0.018	0.008	0.011	0.003	0.001	-
North Sea	0.015	0.009	0.007	0.008	0.016	0.007	0.009	0.003	0.002	0.003

An isolation by distance analysis showed a weak positive association between genetic and geographic distance (Fig. 3.3). A Mantel test failed to show that genetic and geographic distance in *E. tenuis* were correlated ($r = 0.63$, $p > 0.05$).

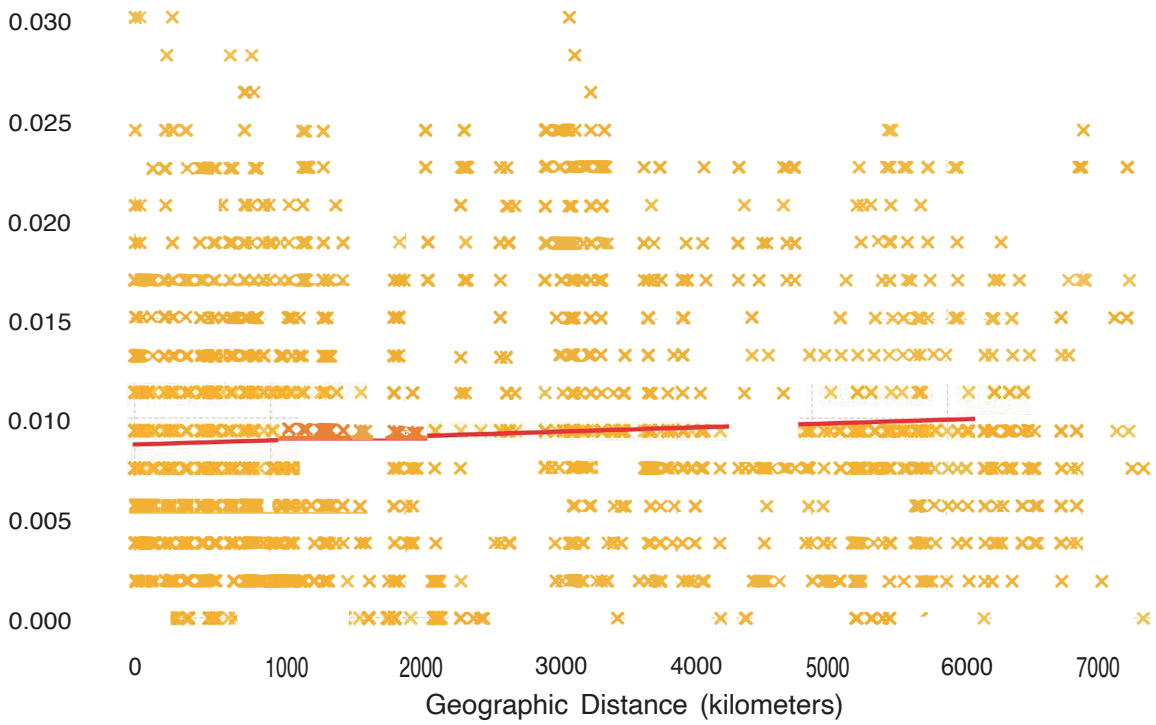


Figure 3.3. A scatterplot of genetic (pairwise F_{st}) and geographic distance (kilometers) of *Ennucula tenuis* specimens from the DBO region and across the Arctic. A red regression line to visualize trend is plotted.

3.3.2 *Macoma calcarea*

Results of the DNA analysis of *M. calcarea* specimens indicated interspecific contamination, with only 1 out of 39 sequences aligning with a published *Macoma* sequences. Using the Basic Local Alignment Search Tool (BLAST) algorithm in the NCBI database, this specimen aligned with another species in the *Macoma* genus, *Macoma moesta* (NCBI, 2025). The DNA of sixteen specimens were an unknown bacterium. Ten specimens aligned closely with human DNA, indicating a probable contamination issue. Ten sequences were a range of bacteria, but with no overlap. These results are detailed in a Appendix Table A2. Further analysis is on-going, and will be reported elsewhere.

3.3.3 *Cistenides hyperborea*

In the DBO region, *C. hyperborea* had two distinct, closely related haplotypes. *C. hyperborea* CO1 mitochondrial fragments showed that these specimens belonged to one population with little genetic diversity (Table 3.7). The Tajima's D statistic was negative, signifying that this gene might be exposed to non-neutral evolution. (Tajima's D = -0.34, Table 3.7) (Tajima, 1989). According to an AMOVA analysis, 100% of diversity was within localities instead of among localities or regions (Table 3.8). Pairwise distance (F_{st}) only showed slight genetic variation between SLIP sites and UTN, SEC, and DBO4 sites (F_{st} = 0.0005; Table 3.9). The median-joining haplotype network displayed two closely related haplotypes within specimens analyzed in this study (Fig. 3.4). In the NCBI, this grouping was most closely related to specimens of *C. granulata* and it is highly divergent from multiple clusters of specimens identified as *C. hyperborea* (Fig. 3.4). Because of high genetic divergence between DBO specimens and the specimens sourced from the NCBI, comparison statistics were not conducted.

Table 3.7. Standard nucleotide indices from *Cistenides hyperborea* CO1 barcode data.

Number of samples	14
Nucleotide diversity	0.0004
Segregating sites	1
Parsimony- informative sites	1
Tajima's D	-0.34
Pairwise-distance	0.00

Table 3.8. Analysis of molecular variance statistics for *Cistenides hyperborea* based on CO1 data.

Source of variation	Sum of squares	Variance components	Percentage variation
Among regions	0	0	0
Among localities within regions	0.286	-0.015	-12.069
Within locality	1.429	0.143	112.069
Total	1.714	0.127	

Table 3.9. Pairwise distance (Fst) *Cistenides hyperborea* CO1 data between sub-regions. Bolded values indicate statistical significance ($p < 0.05$).

	SLIP	UTN	SEC	DBO4
SLIP	-			
UTN	0.001	-		
SEC	0.001	0.000	-	
DBO4	0.001	0.000	0.000	-

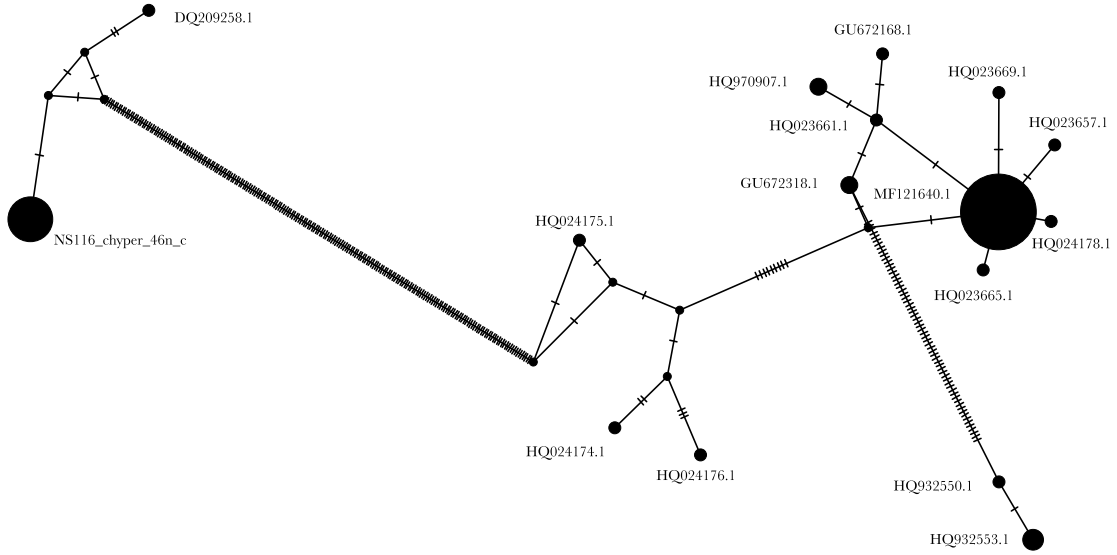


Figure 3.4. Median-joining haplotype network based upon CO1 sequences for *Cistenides hyperborea*. The size of circle represents how many specimens fit into each particular haplotype. Haplotypes. Notches between haplotypes represent one single nucleotide polymorphism (SNP).

3.4 Discussion

Some data support my first hypothesis that DNA barcoding indicated intraspecific diversity not apparent from morphological taxonomy for selected species. The *E. tenuis* specimens analyzed belonged to one population, but there was strong, statistically significant genetic differentiation within the population, including among all sites analyzed in the DBO region ($p < 0.05$, Table 3.5). This diversity was not apparent through taxonomic identification, so genetic analysis increases understanding of apparent intraspecific diversity for this species.

Within the *E. tenuis* population, LB stations in the central Chukchi Sea showed strong differentiation from stations to the south in DBO1 and DBO2 in the northern Bering Sea, and

DBO3 stations in the SE Chukchi Sea. They also showed strong differentiation with NCBI sequences further north in the Beaufort Sea, and east to Igloolik in the Foxe Basin, Hudson Bay and the North Sea (Table 3.6). *Ennucula tenuis* specimens from the Salish Sea (British Columbia, Canada) also showed differentiation from all other sites examined. It is reasonable to conclude that isolation by distance is occurring within this bivalve population, yet there was a weakly positive, but non-significant relationship between genetic and geographic distance (Fig. 3.3). Analyzing more samples from a greater variety of locations in the future could be useful to clarify this potential isolation. *E. tenuis* specimens from the Beaufort Sea were genetically similar to specimens from the North Sea, which supports the idea that isolation by distance is not occurring within this population, which overall has a cosmopolitan distribution.

Life history traits, such as the timing of spawning, could explain genetic divergence observed within this *E. tenuis* population. There also could be an environmental variable or collection of variables driving the divergence of these organisms, but further study is needed. Potentially sediment compositional differences among sites are driving the divergence of these organisms as sediment grain size has been shown to influence biodiversity at the interspecific scale (Grebmeier et al., 1989; Feder et al., 1994; Waga et al., 2020; Chapter 2). Additionally, bottom water salinity during the summer and sediment total organic nitrogen have been shown to drive interspecific biodiversity on the northern Bering and Chukchi shelves (Table 2.6: Section 2.3.3). At certain sites in the DBO, the duration of sea ice persistence has been shown to decrease interspecific biodiversity (Table 2.6: Section 2.3.3). Sea ice persistence may also influence the apparent divergence occurring in this population, especially if it impacts life history traits such as spawning or settlement of *E. tenuis.* Further study of life history characteristics could improve our understanding, in addition to comparing differences among sites, particularly differences in

sediment grain size. Sites showing genetic differences could then be evaluated for potential environmental drivers of divergence in the *E. tenuis* population.

All specimens of *C. hyperborea* collected also belonged to one population, but this population showed little genetic differentiation within the DBO region (Table 3.9). There was likely not a large enough sample size to adequately describe the genetic structure in the DBO regions. When *C. hyperborea* DNA from this study were compared with sequences in the NCBI database, they most closely aligned with a sequence identified as *P. granulata* (Fig. 3.4) (Osborn et al., 2007). *P. granulata* was synonymized or combined with *C. granulata*, which is the currently accepted taxonomic identification. (https://www.marinespecies.org/Carms/aphia.php?p=taxdetails&id=157317). The disparity is only at the species and not genus level (Read and Fauchald, 2021). This cluster was highly divergent from other *P. granulata* specimens in the NCBI. Some of these sequences were from Carr et al. (2011), who found three barcode clusters of *P. granulata* specimens. There is likely some discrepancy in identifications of *P. granulata* and it is also possible that this may be a complex of species, which would benefit from further taxonomic and genetic study. These are challenging species to distinguish (S. Soques, personal communication). One, *C. hyperborea* typically has a range of 12-15 sharp paleae, or spines, while *C. granulata* has a range of 7-13 blunt paleae (Parapar et al., 2020). The haplotype network with specimens from this study and from the NCBI supports the possibility that specimens have been misidentified. Specimens both identified as *C. hyperborea* have more SNPs than would normally be seen for specimens of the same species (Fig. 3.4). These results indicate the importance of ground truthing genetic studies with accurate taxonomy, but also indicates the potential for genetic analyses to aid in studies where species are difficult to identify.

Patterns of differentiation between the Pacific-Arctic, Hudson Bay, and North Sea have been observed in other studies in both mollusk and polychaete populations, indicating that these regions possess distinct populations separated by connectivity breaks (Carr et al., 2011; Layton et al., 2014). Both of these prior studies attributed these differences to the opening and closing of the Bering Strait blocking dispersal in the Pleistocene. Ershova et al. (2019) observed that the meroplankton of the Chukchi Sea is dominated by Pacific expatriates, but that this distribution did not extend north and east into the Beaufort Sea. Thus, there is evidence for high current connectivity between North Pacific and Pacific Arctic shelf macrobenthic populations, but this connectivity does not extend past the Chukchi Sea. My results suggest that *E. tenuis* from the DBO regions are a part of the same population as *E. tenuis* in the Atlantic influenced Arctic margins as well as the Salish Sea in the Pacific Ocean, but with strong signs of genetic differentiation. The negative Tajima's D value suggests that this population will continue expanding genetically, potentially leading to population divergence in the future.

There was not sufficient data to support my second hypothesis; namely that populations of two species (bivalve and polychaete) north of the Bering Strait were not significantly divergent from these populations south of the Strait. The majority of divergence came from within localized populations, both for *E. tenuis* and *C. hyperborea* (Table 3.5, Table 3.8). This result suggests that there are few barriers to gene flow for these two species within the Pacific Arctic region and across the Arctic. Few studies within the DBO region have examined the genetics of benthic macrofaunal invertebrates and so further study is needed. Specifically, expanding analysis to other important/abundant benthic macrofauna in the region would be useful. Given the apparent genomic differences observed in Ledyard Bay (Chukchi Sea), this may be a potentially valuable site to compare with the rest of the DBO study area.

The majority of contaminated *M. calcarea* specimens most closely aligned with contaminated *Limnoria* spp. specimens identified by Hayes et. (2012). This prior study found that analyzed DNA was most closely related to the gut content DNA of the amphipod, *Eurythenes gryllus*, which was contaminated with *Limnoria* spp. (GenBank accession number AY830420). It is likely that contamination in this study is the result of a similar circumstances and it is likely an unidentified bacterium in the gut, possibly living symbiotically with *M. calcarea*. Further analysis through metagenomics could elucidate more about this association, including potentially more information on the feeding patterns of this bivalve, which can both deposit and filter feed (North et al., 2014). Future DNA analysis of *Macoma* spp. in the DBO region should take into consideration the non-target amplification that occurred in this study. This study used a CO1 universal primer amplified a part of the microbial genome, despite CO1 not being a part of that genome. Other studies on *M. calcarea* have had success with the same primer used in this study, so its continued use is warranted (Layton et al., 2014).

Linking accurate biodiversity estimates with environmental dynamics is crucial for understanding how these systems respond to change. An example of this is the study by Galaska et al. (2017) that connected population differences in the brittle star, *Astrotoma agassizii*, with the boundary between the Antarctic Polar Front and Antarctic Circumpolar Current. This study hypothesized that potential changes in hydrography in response to climate change could have implications for Antarctic endemic species. In the Pacific Arctic, currents are typically fast and flow northward through the Bering Strait. This throughflow has been shown to influence many of the environmental properties of the Chukchi Sea (Woodgate, 2018). Pairwise distance analysis of *E. tenuis* in this region appeared to follow a stepwise pattern of differentiation that reflects the currents in this area. Namely, specimens at DBO1 get progressively more genetically different from specimens further north in the DBO2 and DBO3 regions. Areas in the central Chukchi Sea

(Ledyard Bay and to certain extent the more northern DBO4) don't appear to follow this stepwise pattern and are more differentiated from the rest of the DBO regions (Table 3.6). There are two primary currents that flow through the Bering Strait, the Anadyr Current and the Alaska Coastal Water, which are geographically close, but separate water masses that might drive some of these patterns of differentiation. Current speed also plays a role in the composition of sediment size classes in the Chukchi Sea, with coarser sediments generally associated with faster current speeds (Feder et al., 1994), which influences interspecific biodiversity (Grebmeier et al., 1989). Current speed and associated sediment size classes also might influence diversity at the intraspecific scale.

A phylogeographic analysis of two benthic macrofauna, a clam and a polychaete, showed high levels of connectivity in the northern Bering and Chukchi shelves. *C. hyperborea* specimens belonged to one population with little genetic variation, but these sequences differed considerably from *C. hyperborea* sequences in the NCBI. Potential misidentifications at the species level of the same genus, either taxonomically or genetically, need further study. *E. tenuis* specimens belonged to one population, with moderately high levels of divergence geographically. Isolation by distance, or divergence influenced by differences in life history characteristics or environmental variables, was not able to be confirmed. Further study with more specimens analyzed from a wider range of locations, currents and sediment patterns would be promising paths for future research.

Chapter 4. Conclusions: approaching biodiversity in the Pacific Arctic through taxonomic and genetic lenses

4.1 Overview of thesis goals and key findings

4.1.1 Conclusions on Chapter 2: Environmental parameters influencing benthic biodiversity in the Pacific Arctic between 1998 and 2019

Biodiversity increased at DBO sub-regions over the study period 1998 to 2019, specifically at northern Bering Sea stations (SLIP1, SLIP5, UTBS2 and UTBS4) and the SE Chukchi Sea stations (UTN3 and UTN5) (Table 2.5: Section 2.3.3). These increases in biodiversity were found to be driven, in part, by decreases in sea ice observed at each of these stations over the time period (Table 2.6: Section 2.3.3). A shorter annual sea ice persistence was associated with higher biodiversity. Seasonal sea ice loss is likely to continue in this region and so, based on this finding, biodiversity could continue to increase at these sites, and potentially increase at other sites in the region where sea ice is declining.

Ice loss is potentially reducing barriers to expansion for northern Pacific species, thus increasing biodiversity. Future effects on biodiversity are unclear though, as outcomes of interactions between boreal invading and resident species are unknown. Shifts in benthic faunal composition and abundance were observed in the DBO sub-regions. Specifically, there were shifts in dominance from bivalves to polychaetes at sites in the SLIP and UTBS regions in the northern Bering Sea (Fig. 2.2, Fig 2.3: Section 2.3.2). In the DBO3 and DBO4 regions, there was a decline in amphipod abundance and increases in bivalve and polychaete abundance (Fig. 2.4, Fig. 2.5, Fig. 2.6: Section 2.3.3). These shifts in the composition and abundance of the benthos have implications for upper trophic level animals that feed on benthic organisms and play important roles in the food security of indigenous Iñupiat in the region (Moore and Stabeno, 2015).

Decreased ice cover will lead to a greater open water period and increased primary production. This increased primary production could lead to increased consumption in the water column by plankton, less carbon exported to the benthos, and higher macrofaunal biodiversity. Grebmeier et al. (2018) attributed early ice retreat and the timing of the spring phytoplankton bloom to increased organic carbon export to the benthos and increases in benthic biomass at sites in the northern Bering and southern Chukchi Seas. Lower benthic biomass is typically associated with higher benthic biodiversity as greater competition for resources lead to niche differentiation. The proportions and quality of organic carbon export to the benthos, which influences benthic biodiversity, depends on degree of zooplankton grazing in the water column.

The heterogeneity of sediment grain size classes was associated with higher levels of diversity at both regional and sub-regional scales. Only one trend was found in sediment heterogeneity over the time-period of the study, suggesting that it is a relatively stable environmental parameter. This stability could change as increased flow through the Bering Strait related to increases in heat and fresh water has been observed between 2001 and 2014 (Woodgate et al., 2018). Increased current speed is associated with coarser sediments because finer sediments are unable to settle out of the water column. Changes in patterns of sediment distribution will likely affect the composition and biodiversity of benthic habitats.

4.1.2 Conclusions on Chapter 3. Pan-Arctic regional genetic differences of three benthic macrofauna: *Ennucula tenuis*, *Macoma calcarea*, and *Cistenides hyperborea.*

Specimens of the bivalve, *Ennucula tenuis*, and the polychaete, *Cistenides hyperborea*, which were both collected in the DBO study area, belonged to one population for each faunal type. *Ennucula tenuis* showed strong geographic differentiation within the DBO region and *C. hyperborea* showed little genetic differentiation. There are most likely not any oceanographic barriers to the dispersal of these organisms in this region. The geographic genetic differentiation

of *E. tenuis* appeared to be related to limitations in dispersal distance; genetic and geographic distance failed to be correlated in *E. tenuis* specimens analyzed (Fig. 3.3: Section 3.3). This region is influenced by water masses that influence variable patterns of sediment composition, available food supply, and nutrient loads. Specifically, sediment heterogeneity, sediment total organic nitrogen, and bottom water salinity were found to positively influence interspecific biodiversity at the regional scale (Table 2.6: Section 2.3.3). At the sub-regional scale, sea ice persistence was found to negatively influence biodiversity (Table 2.6: Section 2.3.3). It's possible that these environmental parameters are influencing diversity at the intraspecific scale as well. Sediment type is typically associated with particular functional groups of benthic organisms. Potentially, differences in sediment type among sites are driving adaptation and divergence of *E. tenuis*. This clam population is diversifying and so divergence trends seem likely to continue (Table 3.1: Section 3.3).

Cistenides hyperborea specimens analyzed showed little genetic divergence in the DBO region, but were highly divergent from other *C. hyperborea* specimens in the NCBI (Fig. 3.4: Section 3.3). There are known challenges in the taxonomic identification of *Cistenides spp.* specimens, particularly *C. hyperborea* and *C. granulata.* It's possible that there are difficulties in identifying specimens on *C. hyperborea*. These discrepancies between our study and archived genomic data indicates the utility of genetic data in improving the accuracy of identifications especially in morphologically complex cases. This discrepancy also highlights the need for reliable identifications in ecological studies.

4.2 Future Work

The complexity of benthic macrofaunal biodiversity on the Pacific Arctic shelves merit further study. In particular, localities with significant biodiversity trends: the northern Bering Sea (SLIP1, UTBS2) and SE Chukchi Sea stations (UTN3 and SEC2) should be more closely

examined. Different metrics of diversity, such as beta diversity and Simpson's index may provide greater insight into patterns at these stations. Furthermore, because sediment heterogeneity was positively associated with biodiversity and this metric is also a measure of niche differentiation, functional diversity could be further explored, meaning examining biodiversity from the lens what organisms are doing as opposed to individual species. Thus, biological traits that are present in an ecosystem can accomplish important functions, such as the role of bioturbation in mixing sediments and releasing nutrients back into the water column. More biological traits present in an ecosystem (either through overlapping traits or more traits accomplishing more functions), can make the ecosystem more resilient in the face of environmental change. Functional diversity studies in the DBO region could help gain insight into how resilient these habitats are to the rapid climate change occurring. For example, Iken et al. (2020) examined the functional diversity and evenness of the epibenthos in the DBO region and found higher functional diversity at sites in the Beaufort Sea, suggesting that this area might be more resilient to change. Linking environmental influences to functional diversity and examining any change over time would give insight into how these communities might respond to even more additional perturbations. Additionally, knowledge of more detailed life histories on important benthic invertebrates in this area would give insight into ecosystem structure.

More in depth DNA barcoding (>10 specimens per locality) would also be of value for estimates of genetic differences, particularly for *C. hyperborea*, which was sample limited in this study. Furthermore, greater and more even sampling across the entire region, especially in DBO5, would be useful for more accurately describing genetic differentiation observed. Additionally, greater sampling would aid in identifying whether genetic differences are a result of limits in dispersal range, i.e. are geographically based. I was unable to show that genetic

distance was geographically driven, although there was evidence that this was the case (cite your Table or figure that shows this).

Existing collections from the DBO area contain a long and valuable time series record of benthic invertebrates in the region. Implementing a method for extracting DNA for formalin preserved specimens (e.g. Cazzato et al., 2021) would enable the creation of a long time series of genetic data that could be compared with taxonomic records. Connecting these two important measures of biodiversity would be important for predicting resiliency in response to environmental change.

Appendices and supplementary section

Table A1. Sample locations, abbreviations, samples sizes, and collectors of *Ennucula tenuis, Macoma calcarea,* and *Cistenides hyperborea* used in a CO1 DNA barcode analysis. For further information on specimen collections, including cruise and year of collection, refer to supplementary file: **S2. Silverson_popgen2023.csv.**

Location	Station	Number of samples	Sample Origin	Species	Supplementary DNA data file-this study
St. Lawrence Island Polynya, Bering Sea	SLIP4	18	This study	*Ennucula tenuis*	S3_Silverson_e_tenuis_DNA.fasta
Northern Bering Sea	UTBS5	4	This study	*Ennucula tenuis*	S3_Silverson_e_tenuis_DNA.fasta
Southeast Cape, Chukchi Sea	SEC3	2	This study	*Ennucula tenuis*	S3_Silverson_e_tenuis_DNA.fasta
SE Chukchi Sea	UTN7	1	This study	*Ennucula tenuis*	S3_Silverson_e_tenuis_DNA.fasta
Ledyard Bay, Chukchi Sea	LB7	5	This study	*Ennucula tenuis*	S3_Silverson_e_tenuis_DNA.fasta
Barrow Canyon, NE Chukchi Sea	BARC9	1	This study	*Ennucula tenuis*	S3_Silverson_e_tenuis_DNA.fasta
NE Chukchi Sea	DBO4	6	This study	*Ennucula tenuis*	S3_Silverson_e_tenuis_DNA.fasta
Canada: Beaufort Sea, Cape Parry	n/a	6	Layton, et al., 2014	*Ennucula tenuis*	S3_Silverson_e_tenuis_DNA.fasta
Canada: Manitoba, Churchill, Hudson Bay	n/a	4	Layton, et al., 2014	*Ennucula tenuis*	S3_Silverson_e_tenuis_DNA.fasta

Canada: Nunavut, Igloolik	n/a	7	Layton, et al., 2014	*Ennucula tenuis*	S3_Silverson_e_tenuis_DNA.fasta
Greenland: Disko Fjord, Disko Island	n/a	1	Sharma et al., 2013	*Ennucula tenuis*	S3_Silverson_e_tenuis_DNA.fasta
Canada: Newfoundland and Labrador, Nachvak Fjord	n/a	1	Layton, et al., 2014	*Ennucula tenuis*	S3_Silverson_e_tenuis_DNA.fasta
White Sea, Russia	n/a	1	Carr, 2011	*Ennucula tenuis*	S3_Silverson_e_tenuis_DNA.fasta
Sweden: Baltic Sea	n/a	1	Bourlat et al., 2008	*Ennucula tenuis*	S3_Silverson_e_tenuis_DNA.fasta
St. Lawrence Island Polynya, Bering Sea	SLIP4/ SLIP5	7	This study	*Cistenides hyperborea*	S5_Silverson_c_hyperborea_DNA.fasta
Southeast Cape, Chukchi Sea	SEC1/SEC3	3	This study	*Cistenides hyperborea*	S5_Silverson_c_hyperborea_DNA.fasta
SE Chukchi Sea	UTN2	2	This study	*Cistenides hyperborea*	S5_Silverson_c_hyperborea_DNA.fasta
NE Chukchi Sea	DBO4.3n/DBO4.4n/DBO4.5n/DBO4.6n	6	This study	*Cistenides hyperborea*	S5_Silverson_c_hyperborea_DNA.fasta
Barrow Canyon, NE Chukchi Sea	BARC9	2	This study	*Cistenides hyperborea*	S5_Silverson_c_hyperborea_DNA.fasta
St. Lawrence Island Polynya, Bering Sea	SLIP1,2,3,4,5	12	This study	*Macoma calcarea*	S4_Silverson_m_calcarea_DNA.fasta
Southeast Cape, Chukchi Sea	SEC1,2,3	17	This study	*Macoma calcarea*	S4_Silverson_m_calcarea_DNA.fasta

SE Chukchi Sea	UTN2,3,4	7	This study	*Macoma calcarea*	S4_Silverson_m_calcarea_DNA.fasta
NE Chukchi Sea	DBO4.2n, 4.3n, 4.4n, 4.5n	9	This study	*Macoma calcarea*	S4_Silverson_m_calcarea_DNA.fasta

Table A2. Results of a Basic Local Alignment Search Tool (BLAST) algorithm search in the NCBI database for *Macoma calcarea* specimens. Results indicated contamination of DNA sequences of *M. calcarea*.

Specimen ID	Taxonomic ID	BLAST result
NS1	*M. calcarea*	*Candidatus Methylopumilus universalis* isolate
NS2	*M. calcarea*	No result
NS3	*M. calcarea*	*Palaeomystella* sp.
NS5	*M. calcarea*	*Candidatus Thiodubiliella* sp.
NS6	*M. calcarea*	*Homo sapien*
NS7	*M. calcarea*	*Homo sapien*
NS8	*M. calcarea*	*Microbulbifer bruguierae* strain H12
NS11	*M. calcarea*	*Leitoscoloplos pugettensis*
NS12	*M. calcarea*	Uncultured bacterial organism isolate, Hayes et al., 2012
NS13	*M. calcarea*	*Homo sapien*
NS14	*M. calcarea*	Uncultured bacterial organism isolate, Hayes et al., 2012
NS15	*M. calcarea*	*Pseudochrobactrum* sp.
NS16	*M. calcarea*	*Homo sapien*
NS17	*M. calcarea*	Uncultured bacterial organism isolate, Hayes et al.,2012
NS18	*M. calcarea*	Uncultured bacterial organism isolate, Hayes et al.,2012
NS19	*M. calcarea*	*Homo sapien*
NS20	*M. calcarea*	Uncultured bacterial organism isolate, Hayes et al.,2012
NS21	*M. calcarea*	Uncultured bacterial organism isolate, Hayes et al.,2012
NS22	*M. calcarea*	Uncultured bacterial organism isolate, Hayes et al.,2012
NS23	*M. calcarea*	*Homo sapien*
NS24	*M. calcarea*	*Oceanisphaera* sp.
NS25	*M. calcarea*	*Candidatus Thiothrix singaporensis*
NS26	*M. calcarea*	Uncultured bacterial organism isolate, Hayes et al.,2012
NS27	*M. calcarea*	Uncultured bacterial organism isolate, Hayes et al.,2012
NS28	*M. calcarea*	*Pararhizobium* sp.
NS29	*M. calcarea*	Uncultured bacterial organism isolate, Hayes et al.,2012
NS30	*M. calcarea*	Uncultured bacterial organism isolate, Hayes et al.,2012
NS31	*M. calcarea*	Uncultured bacterial organism isolate, Hayes et al.,2012
NS32	*M. calcarea*	Uncultured bacterial organism isolate, Hayes et al.,2012
NS35	*M. calcarea*	*Homo sapien*
NS36	*M. calcarea*	Uncultured bacterial organism isolate, Hayes et al.,2012
NS37	*M. calcarea*	Uncultured bacterial organism isolate, Hayes et al.,2012

NS38	*M. calcarea*	*Homo sapien*
NS40	*M. calcarea*	*Homo sapien*
NS41	*M. calcarea*	*E. tenuis*
NS44	*M. calcarea*	*Homo sapien*
NS45	*M. calcarea*	Uncultured bacterial organism isolate, Hayes et al., 2012
NS46	*M. calcarea*	*M. moesta*
NS47	*M. calcarea*	Uncultured bacterial organism isolate, Hayes et al., 2012

Supplementary data files

S1. Silverson_DBO_diversity2000_2019.csv contains all data used for the statistical analysis of biodiversity in Chapter 2. This data includes Shannon Index, environmental parameters, including sediment variables, from SWL cruises to DBO sites from 2000-2019. Original data available at https://arcticdata.io/catalog/portals/DBO/Data

S2. Silverson_popgen2023.csv lists all collection data for *E. tenuis*, *M. calcarea*, and *C. hyperborea* specimens used in population genetic analyses.

S3. Silverson_e_tenuis_DNA.fasta is a list of aligned and edited DNA for *Ennucula tenuis* specimens.

S4. Silverson_m_calcarea_DNA.fasta is a list of aligned and edited DNA for *Macoma calcarea* specimens. Results indicated contamination of DNA sequences of *M. calcarea* and were inconclusive.

S5. Silverson_c_hyperborea_DNA.fasta is a list of aligned and edited DNA for *Cistenides hyperborea* specimens.

S6. Silverson_NCBI_DNA.fasta is a list of aligned and edited DNA for specimens collected that were not present in the NCBI database, including *Liocyma fluctuosa* (Gould, 1841), *Ocnus glacialis* (Ljungman, 1879), and *Pelonaia corrugata* (Goodsir and Forbes, 1841). Results indicated contamination of DNA sequences of these specimens and were inconclusive.

S7_SWL19_dominance.csv. Summary data as example of dominant benthic macrofaunal for SWL19; original benthic macrofaunal data set available at https://doi.org/10.18739/A2PN8XG88.

S8_Silverson_SWL23_table2023.csv. A summary table of taxa samples for DNA analysis collected on the SWL23 cruise.

S9_Silverson_SKQ202312s_table2023.csv. A summary table of taxa samples for DNA analysis collected on the SKQ2023 cruise.

References

Akaike, H. (1976). Canonical correlation analysis of time series and the use of an information criterion. *System identification* (pp. 27–96). New York: Academic Press.

Alabia, I. D., García Molinos, J., Hirata, T., Mueter, F. J., & David, C. L. (2023). Pan-Arctic marine biodiversity and species co-occurrence patterns under recent climate. *Scientific Reports*, *13*(1), 4076. https://doi.org/10.1038/s41598-023-30943-y

Arrigo, K. R., Perovich, D. K., Pickart, R. S., Brown, Z. W., Van Dijken, G. L., Lowry, K. E., Mills, M. M., Palmer, M. A., Balch, W. M., Bates, N. R., Benitez-Nelson, C. R., Brownlee, E., Frey, K. E., Laney, S. R., Mathis, J., Matsuoka, A., Greg Mitchell, B., Moore, G. W. K., Reynolds, R. A., Swift, J. H. (2014). Phytoplankton blooms beneath the sea ice in the Chukchi sea. *Deep Sea Research Part II: Topical Studies in Oceanography*, 105, 1–16. https://doi.org/10.1016/j.dsr2.2014.03.018

Arrigo, K. R., Perovich, D. K., Pickart, R. S., Brown, Z. W., Van Dijken, G. L., Lowry, K. E., Mills, M. M., Palmer, M. A., Balch, W. M., Bahr, F., Bates, N. R., Benitez-Nelson, C., Bowler, B., Brownlee, E., Ehn, J. K., Frey, K. E., Garley, R., Laney, S. R., Lubelczyk, L., Swift, J. H. (2012). Massive phytoplankton blooms under arctic sea ice. *Science*, 336(6087), 1408–1408. https://doi.org/10.1126/science.1215065

Arrigo, K. R., & Van Dijken, G. L. (2015). Continued increases in Arctic Ocean primary production. *Progress in Oceanography*, 136, 60–70. https://doi.org/10.1016/j.pocean.2015.05.002

Assmy, P., Fernández-Méndez, M., Duarte, P., Meyer, A., Randelhoff, A., Mundy, C. J., Olsen, L. M., Kauko, H. M., Bailey, A., Chierici, M., Cohen, L., Doulgeris, A. P., Ehn, J. K., Fransson, A., Gerland, S., Hop, H., Hudson, S. R., Hughes, N., Itkin, P., Granskog, M. A. (2017). Leads in Arctic pack ice enable early phytoplankton blooms below snow-covered sea ice. *Scientific Reports*, 7(1), 40850. https://doi.org/10.1038/srep40850

Bandelt, H. J., Forster, P., Rohl, A. (1999). Median-joining networks for inferring intraspecific phylogenies. Molecular Biology and Evolution, 16(1), 37–48. https://doi.org/10.1093/oxfordjournals.molbev.a026036

Blanchard, A. L., Parris, C. L., Knowlton, A. L., Wade, N. R. (2013). Benthic ecology of the northeastern Chukchi Sea. Part I. Environmental characteristics and macrofaunal community structure, 2008–2010. *Continental Shelf Research*, 67, 52–66. https://doi.org/10.1016/j.csr.2013.04.021

Carr, C., Hardy, S. M., Brown, T. M., Macdonald, T. A., Hebert, P.D.N. (2010) A tri-oceanic perspective: DNA barcoding reveals geographic structure and cryptic diversity in Canadian polychaetes. *PLoS ONE*, 6: e22232. https://doi.org/10.1371/journal.pone.0022232

Cazzato, G., Caporusso, C., Arezzo, F., Cimmino, A., Colagrande, A., Loizzi, V., Cormio, G., Lettini, T., Maiorano, E., Scarcella, V., Tarantino, P., Marrone, M., Stellacci, A., Parente, P., Romita, P., De Marco, A., Venerito, V., Foti, C., Ingravallo, G., Resta, L. (2021).

Formalin-fixed and paraffin-embedded samples for next generation sequencing: Problems and solutions. *Genes,* 12(10), 1472. https://doi.org/10.3390/genes12101472

Coachman, L. K. (1969). Physical oceanography in the Arctic Ocean: 1968. *Arctic*, *22*(3), 214–224. http://www.jstor.org/stable/40507635

Coachman, L.K., Aagaard K., Tripp, R.B. (1975). Bering Strait: the regional oceanography. *University of Washington Press, Seattle*.

Coan, E.V. (2000). Bivalve Seashells of Western North America: Marine Bivalve Mollusks from Arctic Alaska to Baja California. *1st edition Santa Barbara Museum of Natural History*.

Comiso, J. C., Meier W. N., and Gersten R. (2017). Variability and trends in the Arctic Sea ice cover: Results from different techniques. *Journal of Geophysical Research: Oceans*, 122, 6883-6900, https://doi.org/10.1002/2017JC012768.

Cronin, T.M., Cronin, M.A. (2015). Biological response to climate change in the Arctic Ocean: the view from the past. *Arktos* 1, 4. https://doi.org/10.1007/s41063-015-0019-3

Climate Change: Arctic sea ice summer minimum | NOAA Climate.gov. (n.d.). Retrieved May 10, 2023, from http://www.climate.gov/news-features/understanding-climate/climate-change-arctic-sea-ice-summer-minimum

Dalpadado, P., Arrigo, K. R., Hjøllo, S. S., Rey, F., Ingvaldsen, R. B., Sperfeld, E., Van Dijken, G. L., Stige, L. C., Olsen, A., & Ottersen, G. (2014). Productivity in the Barents Sea—Response to recent climate variability. *PLoS ONE*, 9(5), e95273. https://doi.org/10.1371/journal.pone.0095273

Descôteaux, R., Ershova, E., Wangensteen, O. S., Præbel, K., Renaud, P. E., Cottier, F., & Bluhm, B. A. (2021). Meroplankton diversity, seasonality and life-history traits across the barents sea polar front revealed by high-throughput DNA barcoding. *Frontiers in Marine Science*, 8, 677732. https://doi.org/10.3389/fmars.2021.677732

de la Vega, C., Mahaffey, C., Yurkowski, D. J., Norman, L., Simpson, E., Smout, S., Ferguson, S. H., & Jeffreys, R. M. (2021). Biomarkers in ringed seals reveal recent onset of borealization in the high- compared to the mid-latitude Canadian Arctic. *Frontiers in Marine Science*, 8, 700687. https://doi.org/10.3389/fmars.2021.700687

Dedrick, R.F., Ferron, J.M., Hess, MR, Hogarty, K.Y., Kromrey, J.D., Lang, T.R., Lee, R.S. (2009). Multilevel modeling: a review of methodological issues and applications. Review of Educational Research, 79(1), 69–102. https://doi.org/10.3102/00346543083255

Descamps, S., Strøm, H. (2021). As the Arctic becomes boreal: Ongoing shifts in a high-Arctic seabird community. *Ecology*, 102(11). https://doi.org/10.1002/ecy.3485

Emblemsvåg, M., Pecuchet, L., Velle, L. G., Nogueira, A., Primicerio, R. (2022). Recent warming causes functional borealization and diversity loss in deep fish communities east of

Greenland. *Diversity and Distributions*, 28(10), 2071–2083. https://doi.org/10.1111/ddi.13604

Ershova, E.A., Descoteaux, R., Wangensteen, O.S., Iken, K., Hopcroft, R.R., Smoot, C., Grebmeier, J.M., Bluhm, B.A. (2019). Diversity and distribution of meroplanktonic larvae in the pacific arctic and connectivity with adult benthic invertebrate communities. *Frontiers in Marine Science*, 6, 490. https://doi.org/10.3389/fmars.2019.00490

Excoffier, L., Lischer, H.E.L. (2010). Arlequin suite ver 3.5: A new series of programs to perform population genetics analyses under Linux and Windows. *Molecular Ecology Resources*, 10(3), 564–567. https://doi.org/10.1111/j.1755-0998.2010.02847.x

Feder, H.M., Naidu, A.S., Jewett, S.C., Hameedi, J.M., Johnson, W.R., Whitledge, T.E. (1994). The northeastern Chukchi Sea: benthos–environmental interactions. *Marine Ecology Progress Series*, 111, 171–190.

Feder, H.M., Jewett, S.C., Blanchard, A. (2007). Southeastern Chukchi Sea (Alaska) macrobenthos. *Polar Biology* 30, 261–275.

Fernández-Méndez, M., Katlein, C., Rabe, B., Nicolaus, M., Peeken, I., Bakker, K., Flores, H., Boetius, A. (2015). Photosynthetic production in the central Arctic Ocean during the record sea-ice minimum in 2012. *Biogeosciences*, 12(11), 3525–3549. https://doi.org/10.5194/bg-12-3525-2015

Frankham, R. (2005). Genetics and extinction. *Biological Conservation*, 126(2), 131-140. https://doi.org/10.1016/j.biocon.2005.05.002

Fossheim, M., Primicerio, R., Johannesen, E., Ingvaldsen, R.B., Aschan, M.M., Dolgov, A.V. (2015). Recent warming leads to a rapid borealization of fish communities in the Arctic. *Nature Climate Change*, 5(7), 673–677. https://doi.org/10.1038/nclimate2647

Fox, J. (2016) Applied Regression Analysis and Generalized Linear Models, Third Edition. Sage.

Frey, K.E., Comiso, J.C., Stock, L.V., Young, L.N.C., Cooper, L.W., Grebmeier, J.M. (2023). A comprehensive satellite-based assessment across the Pacific Arctic Distributed Biological Observatory shows widespread late-season sea surface warming and sea ice declines with significant influences on primary productivity. *PLoS ONE*, 18(7), e0287960. https://doi.org/10.1371/journal.pone.0287960

Fuertes, A. (2008). Sieve bootstrap t-tests on long-run average parameters. *Computational Statistics & Data Analysis*, Elsevier, vol. 52(7), pages 3354-3370, March.

Forbes, E., Goodsir, J. (1841). On Pelonaia, a new genus of tunicated mollusks, with description of two species. *New Philosophical Journal, Edinburgh*. 31, 29-34. https://books.google.be/books?id=rGo7AQAAIAAJ&pg=PA29&lpg=PA29&dq=On+Pelonaia,+a+new+genus+of+tunicated+mollusks,+with+description+of+two+species&source=bl

&ots=NgY3sPoRb1&sig=QwE9S4362qrM-8wQNqIKEtcQYl8&hl=pt-PT&sa=X&ved=2ahUKEwiW4cuK8PPcAhUKbVAKHQhjDbMQ6 [details]

Galaska, M.P., Sands, C.J., Santos, S.R., Mahon, A.R., Halanych, K.M. (2017a). Crossing the divide: Admixture across the antarctic polar front revealed by the brittle star *Astrotoma agassizii*. The Biological Bulletin, 232(3), 198–211. https://doi.org/10.1086/693460

Galaska, M.P., Sands, C.J., Santos, S.R., Mahon, A.R., Halanych, K.M. (2017b). Geographic structure in the Southern Ocean circumpolar brittle star *Ophionotus victoriae* (Ophiuridae) revealed from mt DNA and single-nucleotide polymorphism data. Ecology and Evolution, 7(2), 475–485. https://doi.org/10.1002/ece3.2617

Geraldi, N.R., Krause-Jensen, D., Ørberg, S.B., Frühe, L., Sejr, M.K., Hansen, J.L.S., Lund-Hansen, L., Duarte, C. M. (2024). Environmental drivers of Arctic communities based on metabarcoding of marine sediment eDNA. *Proceedings of the Royal Society B: Biological Sciences*, 291(2015), 20231614. https://doi.org/10.1098/rspb.2023.1614

Gould, A.A. (1841). Report on the Invertebrata of Massachusetts, Comprising the Mollusca, Crustacea, Annelida, and Radiata. Published Agreeably to an Order of the Legislature, by the *Commissioners on the Zoological and Botanical Survey of the State. Folsom, Wells, and Thurston*. http://www.biodiversitylibrary.org/item/76081

Gmelin J.F. (1791). Caroli a Linnaei Systema Naturae per Regna Tria Naturae, Ed. 13. Tome 1(6). G.E. Beer, Lipsiae [Leipzig]. pp. 3021-3910. *Systema Naturae*, 13(1).

Good, I. J. (1953). The population frequencies of species and the estimation of population parameters. *Biometrika*, 40(3–4), 237–264. https://doi.org/10.1093/biomet/40.3-4.237

Goldsmit, J., McKindsey, C.W., Schlegel, R.W., Stewart, D.B., Archambault, P., Howland, K.L. (2020). What and where? Predicting invasion hotspots in the Arctic marine realm. *Global Change Biology*, 26(9), 4752–4771. https://doi.org/10.1111/gcb.15159

Grebmeier, J., Feder, H., McRoy, C. (1989). Pelagic-benthic coupling on the shelf of the northern Bering and Chukchi Seas. II. Benthic community structure. *Marine Ecology Progress Series*, 51, 253–268. https://doi.org/10.3354/meps051253

Grebmeier, J. M., Cooper, L. W., Feder, H. M., & Sirenko, B. I. (2006a). Ecosystem dynamics of the pacific-influenced northern Bering and Chukchi Seas in the Amerasian Arctic. *Progress in Oceanography*, 71(2–4), 331–361. https://doi.org/10.1016/j.pocean.2006.10.001

Grebmeier, J.M., Overland, J.E., Moore, S.E., Farley, E.V., Carmack, E.C., Cooper, L.W., Frey, K.E., Helle, J.H., McLaughlin, F.A., McNutt, S.L. (2006b). A major ecosystem shift in the northern Bering sea. *Science*, 311(5766), 1461–1464. https://doi.org/10.1126/science.1121365

Grebmeier, J.M., Bluhm, B.A., Cooper, L.W., Danielson, S.L., Arrigo, K.R., Blanchard, A.L., Clarke, J.T., Day, R.H., Frey, K.E., Gradinger, R.R., Kędra, M., Konar, B., Kuletz, K.J., Lee, S.H., Lovvorn, J.R., Norcross, B.L., Okkonen, S.R. (2015). Ecosystem characteristics

and processes facilitating persistent macrobenthic biomass hotspots and associated benthivory in the Pacific Arctic. *Progress in Oceanography*, 136, 92–114. https://doi.org/10.1016/j.pocean.2015.05.006

Grebmeier, J., Frey, K., Cooper, L., & Kędra, M. (2018). Trends in benthic macrofaunal populations, seasonal sea ice persistence, and bottom water temperatures in the Bering Strait region. *Oceanography*, 31(2). https://doi.org/10.5670/oceanog.2018.224

Hansell, DA., Whitledge, T. E., Goering, J.J. (1993). Patterns of nitrate utilization and new production over the Bering-Chukchi shelf. *Continental Shelf Research*, 13(5–6), 601–627. https://doi.org/10.1016/0278-4343(93)90096-G

Hardy, S.M., Carr, C.M., Hardman, M., Steinke, D., Corstorphine, E., Mah, C. (2011). Biodiversity and phylogeography of Arctic marine fauna: Insights from molecular tools. *Marine Biodiversity*, 41(1), 195–210. https://doi.org/10.1007/s12526-010-0056-x

Hebert, P.D.N., Cywinska, A., Ball, S.L., deWaard, J.R. (2003). Biological identifications through DNA barcodes. *Proceedings of the Royal Society of London. Series B: Biological Sciences*, 270(1512), 313–321. https://doi.org/10.1098/rspb.2002.2218

Kędra, M., Grebmeier, J.M. (2021). Ecology of Arctic Shelf and Deep Ocean Benthos. In D. N. Thomas (Ed.), *Arctic Ecology* (1st ed., pp. 325–355). Wiley. https://doi.org/10.1002/9781118846582.ch12

Koch, C. W., Cooper, L. W., Lalande, C., Brown, T. A., Frey, K. E., & Grebmeier, J. M. (2020). Seasonal and latitudinal variations in sea ice algae deposition in the Northern Bering and Chukchi Seas determined by algal biomarkers. *PLoS ONE*, 15(4), e0231178. https://doi.org/10.1371/journal.pone.0231178

Kohlbach, D., Graeve, M., A. Lange, B., David, C., Peeken, I., & Flores, H. (2016). The importance of ice algae-produced carbon in the central Arctic Ocean ecosystem: Food web relationships revealed by lipid and stable isotope analyses: Ice algal carbon in Arctic food web. *Limnology and Oceanography*, 61(6), 2027–2044. https://doi.org/10.1002/lno.10351

Konopiński, M. K. (2020). Shannon diversity index: A call to replace the original Shannon's formula with unbiased estimator in the population genetics studies. *PeerJ*, 8, e9391. https://doi.org/10.7717/peerj.9391

Kortsch, S., Primicerio, R., Beuchel, F., Renaud, P.E., Rodrigues, J., Lønne, O.J., Gulliksen, B. (2012). Climate-driven regime shifts in Arctic marine benthos. P*roceedings of the National Academy of Sciences*, 109(35), 14052–14057. https://doi.org/10.1073/pnas.1207509109

Lannuzel, D., Tedesco, L., Van Leeuwe, M., Campbell, K., Flores, H., Delille, B., Miller, L., Stefels, J., Assmy, P., Bowman, J., Brown, K., Castellani, G., Chierici, M., Crabeck, O., Damm, E., Else, B., Fransson, A., Fripiat, F., Geilfus, N.X., Wongpan, P. (2020). The future of Arctic sea-ice biogeochemistry and ice-associated ecosystems. *Nature Climate Change*, 10(11), 983–992. https://doi.org/10.1038/s41558-020-00940-4

Layton K.K., Martel A.L., Hebert P.D. (2014) Patterns of DNA Barcode Variation in Canadian Marine Molluscs. *PLoS ONE* 9(4), e95003. https://doi.org/10.1371/journal.pone.0095003

Leigh, J. W., Bryant, D. (2015). popart: Full-feature software for haplotype network construction. *Methods in Ecology and Evolution*, 6(9), 1110–1116. https://doi.org/10.1111/2041-210X.12410

Lindstrom, M.J., Bates, D.M. (1988). Newton-Raphson and EM Algorithms for Linear Mixed-Effects Models for Repeated-Measures Data. *Journal of the American Statistical Association* 83, 1014–1022. doi:10.2307/2290128.

Lin, H., Liu, K., Wang, J., Lin, J., Huang, Y., He, X., Li, Z., Zhang, S., Mou, J., Liu, Y., Song, P., Wang, Y., Xing, B. (2019). Spatial Variability of Macrobenthic Production in the Bering Sea. *Polar Biology*. 42 (3), 449–60. https://doi.org/10.1007/s00300-018-2414-2.

Ljungsman, AW. (1879). Fötrteckning öfver Spetsbergens Holothurider. *Ofversigt Kongliga Svenska Vetenskaps-Akademiens Forhandlingar*. 46, 127-131.

Macias-Fauria, M., Post, E. (2018). Effects of sea ice on Arctic biota: An emerging crisis discipline. *Biology Letters*, 14(3). https://doi.org/10.1098/rsbl.2017.0702

Maestrini, L., Hui, F.K.C., Welsh, A.H. (2024). Restricted maximum likelihood estimation in generalized linear mixed models. *arXiv*. https://doi.org/10.48550/ARXIV.2402.12719

Margalef, R. 1957. La teoría de la información en Ecología. *Memorias de la Real Academia de Ciencias y Artes de Barcelona,* 32373–436.

Maslanik, J., Stroeve, J., Fowler, C., & Emery, W. (2011). Distribution and trends in Arctic sea ice age through spring 2011. *Geophysical Research Letters*, 38(13). https://doi.org/10.1029/2011GL047735

Meier, W. N., Hovelsrud, G. K., Van Oort, B. E. H., Key, J. R., Kovacs, K. M., Michel, C., Haas, C., Granskog, M. A., Gerland, S., Perovich, D. K., Makshtas, A., & Reist, J. D. (2014). Arctic sea ice in transformation: A review of recent observed changes and impacts on biology and human activity. *Reviews of Geophysics*, 52(3), 185–217. https://doi.org/10.1002/2013RG000431

Montagu, G. (1808). Supplement to Testacea Britannica with Additional Plates. Woolmer, Exeter. 183, pl.17-30. https://www.biodiversitylibrary.org/page/61685744

Moore, S.E., Grebmeier, J.M. (2018). The Distributed Biological Observatory: Linking physics to biology in the Pacific arctic region. *ARCTIC*, 71(5). https://doi.org/10.14430/arctic4606

Moore, S.E., Grebmeier, J.M., Davies, J.R. (2003). Gray whale distribution relative to forage habitat in the northern Bering Sea: Current conditions and retrospective summary. *Canadian Journal of Zoology*, 81(4), 734–742. https://doi.org/10.1139/z03-043

Moore, S.E., Logerwell, E., Eisner, L., Farley, E.V., Harwood, L.A., Kuletz, K., Lovvorn, J., Murphy, J. R., Quakenbush, L.T. (2014). Marine fishes, birds and mammals as sentinels of ecosystem variability and reorganization in the pacific arctic region. In J. M. Grebmeier & W. Maslowski (Eds.), The Pacific Arctic Region (pp. 337–392). Springer Netherlands. https://doi.org/10.1007/978-94-017-8863-2_11

Moore, S. E., Stabeno, P.J. (2015). Synthesis of arctic research (Soar) in marine ecosystems of the pacific arctic. *Progress in Oceanography*, 136, 1–11. https://doi.org/10.1016/j.pocean.2015.05.017

Mueter, F.J., Iken, K., Cooper, L.W., Grebmeier, J.M., Kuletz, K.J., Hopcroft, R.R., Danielson, S.L., Collins, R.E., Cushing, D.A. (2021). Changes in diversity and species composition across multiple assemblages in the Eastern Chukchi Sea during two contrasting years are consistent with borealization." *Oceanography*, 34 (2). https://doi.org/10.5670/oceanog.2021.213

Møller, E.F., Nielsen, T.G. (2020). Borealization of Arctic zooplankton—Smaller and less fat zooplankton species in Disko Bay, Western Greenland. *Limnology and Oceanography*, 65(6), 1175–1188. https://doi.org/10.1002/lno.11380

Moore, S.E., Stabeno, P.J. (2015). Synthesis of arctic research (SOAR) in marine ecosystems of the Pacific Arctic. *Progress in Oceanography*, 136, 1–11. https://doi.org/10.1016/j.pocean.2015.05.017

Nelson, R., Carmack, E., McLaughlin, F., Cooper, G. (2009). Penetration of Pacific zooplankton into the western Arctic Ocean tracked with molecular population genetics. *Marine Ecology Progress Series*, 381, 129–138. https://doi.org/10.3354/meps07940

Osborne, E., Cronin, T., Farmer J. (2017). Paleoceanographic perspectives on Arctic ocean change. *NOAA Arctic Research*. https://arctic.noaa.gov/Report-Card/Report-Card-2017/ArtMID/7798/ArticleID/690/Paleoceanographic-Perspectives-on-Arctic-Ocean-Change

Parapar, J., Palomanes, V., Helgason, G.V., Moreira, J. (2020). Taxonomy and distribution of Pectinariidae (Annelida) from Iceland with a comparative analysis of uncinal morphology. *European Journal of Taxonomy*, 666. https://doi.org/10.5852/ejt.2020.666

Pecuchet, L., Blanchet, M., Frainer, A., Husson, B., Jørgensen, L.L., Kortsch, S., Primicerio, R. (2020). Novel feeding interactions amplify the impact of species redistribution on an Arctic food web. *Global Change Biology*, 26(9), 4894–4906. https://doi.org/10.1111/gcb.15196

Pisareva, M., Pickart, R., Iken, K., Ershova, E., Grebmeier, J., Cooper, L., Bluhm, B., Nobre, C., Hopcroft, R., Hu, H., Wang, J., Ashjian, C., Kosobokova, K., Whitledge, T. (2015). The relationship between patterns of benthic fauna and zooplankton in the Chukchi sea and physical forcing. *Oceanography*, 28(3), 68–83. https://doi.org/10.5670/oceanog.2015.58

Polyakov, I.V., Alkire, M.B., Bluhm, B.A., Brown, K.A., Carmack, E.C., Chierici, M., Danielson, S.L., Ellingsen, I., Ershova, E.A., Gårdfeldt, K., Ingvaldsen, R.B., Pnyushkov,

A.V., Slagstad, D., Wassmann, P. (2020). Borealization of the Arctic Ocean in response to anomalous advection from sub-arctic seas. *Frontiers in Marine Science*, 7, 491. https://doi.org/10.3389/fmars.2020.00491

Post, E., Forchhammer, M.C., Bret-Harte, M.S., Callaghan, T.V., Christensen, T.R., Elberling, B., Fox, A.D., Gilg, O., Hik, D.S., Høye, T.T., Ims, R.A., Jeppesen, E., Klein, D.R., Madsen, J., McGuire, A.D., Rysgaard, S., Schindler, D.E., Stirling, I., Tamstorf, M.P., Aastrup, P. (2009). Ecological dynamics across the Arctic associated with recent climate change. *Science*, 325 (5946), 1355–1358. https://doi.org/10.1126/science.1173113

Renaud, P.E., Sejr, M.K., Bluhm, B.A., Sirenko, B., Ellingsen, I.H. (2015). The future of Arctic benthos: Expansion, invasion, and biodiversity. *Progress in Oceanography*, 139, 244–257. https://doi.org/10.1016/j.pocean.2015.07.007

Renaud, P.E., Wallhead, P., Kotta, J., Włodarska-Kowalczuk, M., Bellerby, R.G.J., Rätsep, M., Slagstad, D., Kukliński, P. (2019). Arctic sensitivity? Suitable habitat for benthic taxa is surprisingly robust to climate change. *Frontiers in Marine Science*, 6, 538. https://doi.org/10.3389/fmars.2019.00538

Roy V., Iken K., Archambault, P. (2014) Environmental drivers of the Canadian Arctic megabenthic communities. *PLoS ONE* 9(7): e100900. https://doi.org/10.1371/journal.pone.0100900

Sanger, F., Nicklen, S., Coulson, A.R. (1977). DNA sequencing with chain-terminating inhibitors. *Proceedings of the National Academy of Sciences*, 74(12), 5463–5467. https://doi.org/10.1073/pnas.74.12.5463

Sirenko, B.I., Gagaev, S. (2007). Unusual abundance of macrobenthos and biological invasions in the Chukchi Sea. *Russian Journal of Marine Biology*, 33(6), 355–364. https://doi.org/10.1134/S1063074007060016

Shannon, C.E. (1948). A mathematical theory of communication. *Bell System Technical Journal*, 27(3), 379–423. https://doi.org/10.1002/j.1538-7305.1948.tb01338.x

Solan, M., Cardinale, B.J., Downing, A.L., Engelhardt, K.A.M., Ruesink, J.L., Srivastava, D.S. (2004). Extinction and ecosystem function in the marine benthos. *Science*, 306(5699), 1177–1180. https://doi.org/10.1126/science.1103960

Sonet, G., Smitz, N., Vangestel, C., Samyn, Y. (2022). DNA barcoding echinoderms from the East Coast of South Africa. The challenge to maintain DNA data connected with taxonomy. *PLoS ONE* 17(10): e0270321. https://doi.org/10.1371/journal. pone.0270321

Springer, A.M., McRoy, C.P., Flint, M.V. (1996). The Bering Sea Green Belt: Shelf-edge processes and ecosystem production. *Fisheries Oceanography*, 5(3–4), 205–223. https://doi.org/10.1111/j.1365-2419.1996.tb00118.x

Sutton, L., Iken, K., Bluhm, B., Mueter, F. (2020). Comparison of functional diversity of two Alaskan Arctic shelf epibenthic communities. *Marine Ecology Progress Series*, 651, 1–21. https://doi.org/10.3354/meps13478

Tamura, K., Stecher, G., Kumar, S. (2021). Mega11: Molecular evolutionary genetics analysis version 11. *Molecular Biology and Evolution,* 38(7), 3022–3027. https://doi.org/10.1093/molbev/msab120

Thaler, M., Labarre, A., Lovejoy, C. (2024). Environmental selection and advective transport shape the distribution of two cyst-forming Acantharia clades in the Canadian Arctic. *Journal of Plankton Research*, fbae051. https://doi.org/10.1093/plankt/fbae051

Van Den Heuvel-Greve, M.J., Van Den Brink, A.M., Glorius, S.T., De Groot, G.A., Laros, I., Renaud, P.E., Pettersen, R., Węsławski, J.M., Kuklinski, P., Murk, A.J. (2021). Early detection of marine non-indigenous species on Svalbard by DNA metabarcoding of sediment. *Polar Biology*, 44(4), 653–665. https://doi.org/10.1007/s00300-021-02822-7

Vermeij, G. J., Roopnarine, P.D. (2008). The coming Arctic invasion. *Science*, 321(5890), 780–781. https://doi.org/10.1126/science.1160852

Waga, H., Hirawake, T., Grebmeier, J.M. (2020). Recent change in benthic macrofaunal community composition in relation to physical forcing in the Pacific Arctic. *Polar Biology*, 43(4), 285–294. https://doi.org/10.1007/s00300-020-02632-3

Woodgate, R. A. (2018). Increases in the Pacific inflow to the Arctic from 1990 to 2015, and insights into seasonal trends and driving mechanisms from year-round Bering Strait mooring data. *Progress in Oceanography*, 160, 124–154. https://doi.org/10.1016/j.pocean.2017.12.007

Ye, J., Xiao, C., Esteves, R.M., Rong, C. (2015). Time Series Similarity Evaluation Based on Spearman's Correlation Coefficients and Distance Measures. In: Qiang, W., Zheng, X., Hsu, CH. (eds) Cloud Computing and Big Data. CloudCom-Asia 2015. *Lecture Notes in Computer Science*, vol 9106. Springer, Cham. https://doi.org/10.1007/978-3-319-28430-9_24